WORKSHOP ON COSMOGENIC NUCLIDES

Los Alamos National Laboratory
and
Lunar and Planetary Institute

26-27 July 1984

PROGRAM

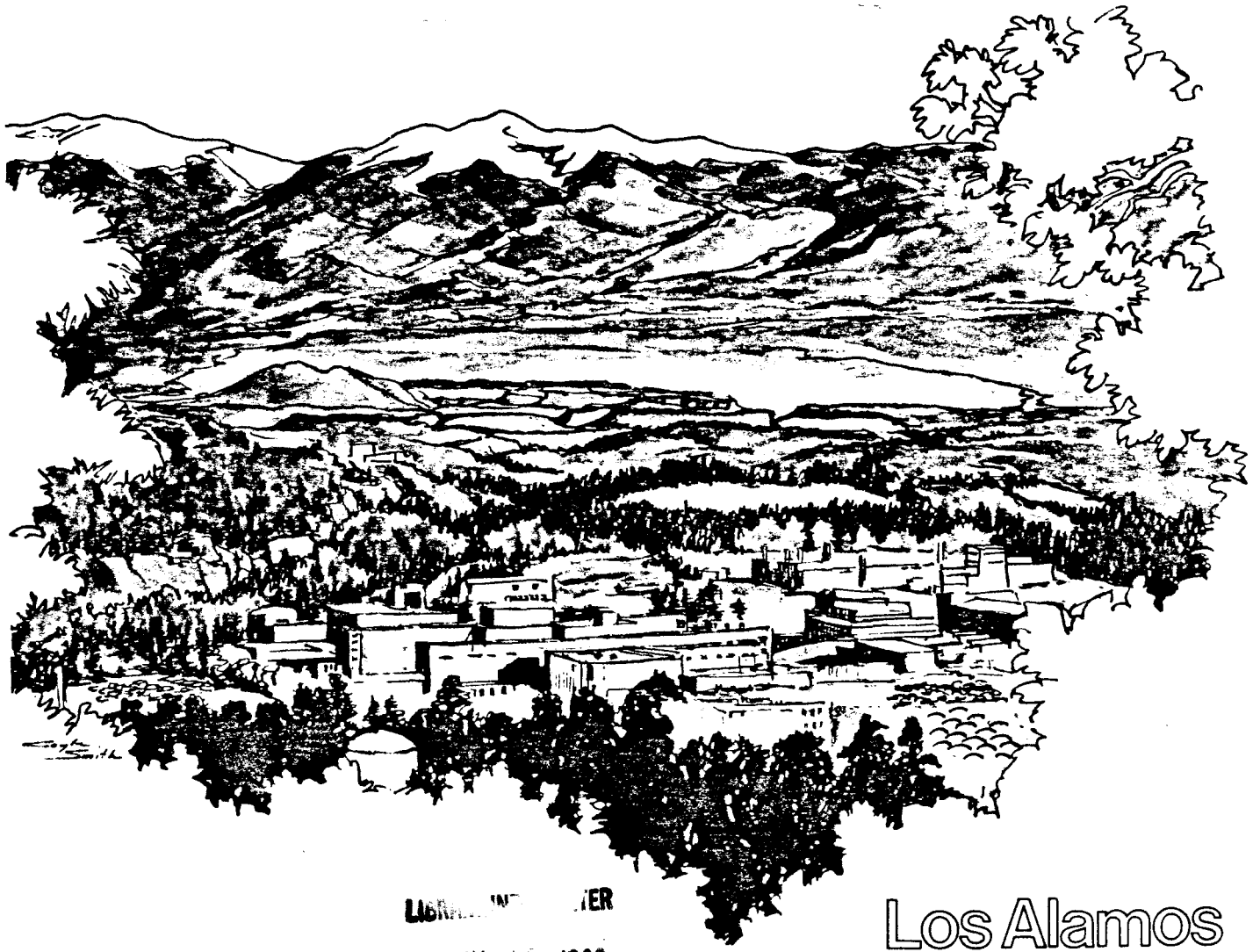

Los Alamos
Los Alamos National Laboratory
Los Alamos, New Mexico 87545

WORKSHOP ON COSMOGENIC NUCLIDES, Thursday, 26 July 1984

Los Alamos National Laboratory, Los Alamos, New Mexico

INC-DO Conference Room, Tech Area 48, Building RC-29

8:15 a.m. Bus from Los Alamos Inn to TA-48

8:30 a.m. Registration at TA-48

8:45 a.m. Opening Activities

R. C. Reedy, General Comments about the Workshop

D. C. Hoffman, INC-DO, Welcome

J. R. Arnold, A review of the history of cosmogenic nuclides.

BREAK

9:30 a.m. New Techniques for Measuring Cosmogenic Nuclides

D. Rokop, "Measuring a Small Number of Atoms - The Pitfall of Isobaric Impurities."

C. M. Miller, "Resonance Ionization Mass Spectrometry for Isotopic Abundance Measurements."

U. Fehn, D. Elmore, H. E. Gove, P. Kubik, R. Teng, and L. Tubbs, "Determination of Ca-41, I-129 and Os-187 in the Rochester Tandem Accelerator and Some Applications of These Isotopes."

A. J. T. Jull, D. J. Donahue, and T. H. Zabel, "Radionuclide Measurements by Accelerator Mass Spectrometry at Arizona."

11:30 a.m. Bus leaves for cafeteria in Otowi Building

12:45 p.m. Bus leaves cafeteria for TA-48

1:00 p.m. Solar Modulation

M. A. Forman (to be presented by R. Zwickl), "Solar Modulation of Galactic Cosmic Rays: Contemporary Observations and Theories."

1:45 p.m. Terrestrial Studies

K. O'Brien, "Calculations of Cosmogenic Nuclide Production Rates in the Earth's Atmosphere and their Inventories."

D. Lal (to be presented by J. Goswami), "Cosmic Ray Interactions in the Ground: Temporal Variations in Cosmic Ray Intensities and Geophysical Studies."

BREAK

3:00 p.m. Simulations and Cross Sections

J. Brückner, P. Englert, R. C. Reedy, and H. Wänke, "Simulation Experiments for Gamma-Ray Mapping of Planetary Surfaces: Scattering of High-Energy Neutrons."

S. Theis, P. Englert, R. C. Reedy, and J. R. Arnold, "Simulation of Cosmic Irradiation Conditions in Thick Target Arrangements."

R. Michel, P. Dragovitsch, P. Englert, and U. Herpers, "Production of Radionuclides in Artifical Meteorites Irradiated Isotropically with 600 MeV Protons."

D. A. Leich, R. J. Borg, and V. B. Lanier, "Production Rates of Neon and Xenon Isotopes by Energetic Neutrons."

5:15 p.m. Bus leaves for Dinner in Otowi Building

5:30 p.m. Hors d'oeuvres and wine on Otowi Building patio

6:15 p.m. Workshop Dinner in Otowi Building

8:00 p.m. Bus goes to Los Alamos Inn

Friday, 27 July 1984

J. Robert Oppenheimer Study Center, TA-3, Upper Floor

8:15 a.m. Bus leaves Los Alamos Inn for Study Center

8:30 a.m. Calculations for Extraterrestrial Matter

M. S. Spergel, R. C. Reedy, O. W. Lazareth, and P. W. Levy, "Neutron Capture Production Rates of Cosmogenic Co-60, Ni-59 and Cl-36 in Stony Meteorites."

L. E. Nyquist and A. F. McDowell, "Redetermination of Parameters for Semi-Empirical Model for Spallogenic He and Ne in Chondrites."

BREAK

9:45 p.m. Meteorites

M. W. Caffee, J. N. Goswami, C. M. Hohenberg, and T. D. Swindle, "Precompaction Irradiaton Effects: Particles from an Early Active Sun?"

J. N. Goswami, "Evolution of Gas-Rich Meteorites: Clues from Cosmogenic Nuclides."

J. R. Arnold and K. Nishiizumi, "Nuclide Production in (Very) Small Meteorites."

R. Sarafin, U. Herpers, P. Englert, R. Wieler, P. Signer, G. Bonani, M. Nessi, M. Suter, and W. Wölfli, "Studies on Cosmogenic Nuclides in Meteorites with Regard to an Application as Potential Depth Indicators."

11:45 a.m. Lunch in Otowi cafeteria (side rooms reserved for Workshop)

1:00 p.m. Meteorites (continued)

R. Wieler, P. Signer, U. Herpers, R. Sarafin, G. Bonani, H. J. Hofmann, E. Morenzoni, M. Nessi, M. Suter, and W. Wölfli, "Spallogenic Nuclides in a Cross Section of Knyahinya."

G. Heusser, "The Exposure History of Jilin and Production Rates of Cosmogenic Nuclides."

L. Schultz and M. Freundel, "The Production Rate of Cosmogenic 21-Ne in Chondrites Deduced from 81-Kr Measurements."

BREAK

D. K. Pal, C. Tuniz, R. K. Moniot, W. Savin, S. Vajda, T. Kruse, and G. F. Herzog, "Be-10 Contents of SNC Meteorites."

K. Nishiizumi, "Compilation of Cosmogenic Radionuclides in Meteorites."

5:00 p.m. Bus goes to Los Alamos Inn

added talk by R. O. Pepin

Workshop on Cosmogenic Nuclides

Jan 5679

NAME	Amt. Paid	No. for Dinner	Workshop fee	
✓ ~~Arnold, J.-UCSD~~	$27.50 12.50 40.00 27.50	~~2~~	x	
✓ Birck, J. - U. Paris		1	x	
✓ Brueckner, J. - MPI-Mainz	27.50	1	x	
✓ Caffee, M. - Wash. U.	27.50	1	x	
✓ Crozaz, G. - Wash. U.	27.50	1	x	
✓ Eberhard, P.	27.50	1	x	
✓ Englert, P. - U. Cologne	40.00	1	x	($12.50)
✓ Fehn, U., - U. Rochester	40.00	2	x	1 child
~~Forman, M. - SUNY-Stony Brook~~				
✓ Goswami, J.- PRL India	27.50	1	x	
✓ Herpers, U. - U. Cologne	40.00	2	x	
✓ Herzog, G. - Rutgers U.	12.50 15.00 27.50	1	x	
✓ Heusser, G. - MPI-Heidelberg	65.00	4	x	2 children (teen)
✓ Hohenberg, C. - Wash. U.	27.50	1	x	
✓ Jones, P. - LPI	12.50	1	-	
✓ Jull, T. - U. Ariz.	27.50	1	x	
✓ Leavy, B.	27.50	1	x	
✓ Leich, D. - LLNL	27.50	1	x	
✓ Marti, K. - UCSD ($30.00 prev. pd.)	35.00	4	x	~~2 children~~ 2 children (teens)
~~McDowell, P.~~				
✓ Miller, C. - LANL				
✓ Nautiyal, C. - PRL India	27.50	1	x	
✓ Nishiizumi, K. - UCSD	27.50	1	x	
✓ Nyguist, L. - UCSD	27.50	1	x	
✓ O'Brien, K. - DOE EML	27.50	1	x	
✓ Ott, U. - MPI-Mainz	27.50	1	x	
✓ Pepin, R. - U. Minnesota	27.50	1	x	
✓ Phillips / ~~Poths, J.-LANL~~				
✓ Reedy, R. - LANL		1		

Workshop on Cosmogenic Nuclides

NAME	Amt. Paid.	No. for Dinner	Workshop fee	
✓ Regnier, S - Bordeaux	27.50	1	X	
✓ Sarafin, R - U. Cologne	$27.50	1	x	
✓ Schultz, L. - MPI-Mainz	27.50	1	X	
~~Signer, P. ETH Zurich~~				
✓ Simonoff, G. - Bordeaux	55.00	1	X	
✓ Simonoff, M. - Bordeaux		1	X	
✓ Sonett, C. -	27.50	1	X	
✓ Spergel, M. - Cuny & BNL	27.50	1	x	
✓ Swindle, Wash. U.	15.00		X	
✓ Tazawa, Y. - Kyoto	27.50	1	X	
Velsko, C. - LLNL	27.50	1	x	
✓ Wieler, R. - ETH Zurich	28.00	1	x	($.50) pd

44

Papers Presented to the
Workshop on Cosmogenic Nuclides

Sponsored by

Los Alamos National Laboratory
and
Lunar and Planetary Institute

Hosted by

Los Alamos National Laboratory
at New Mexico
July 26-27, 1984

TABLE OF CONTENTS

NUCLIDE PRODUCTION IN (VERY) SMALL METEORITES; James R. Arnold and Kunihiko Nishiizumi, Dept. of Chemistry, Univ. of Calif., San Diego, La Jolla, CA 92093.

One of the most interesting open questions in the study of cosmic-ray effects in meteorites is the expected behavior of objects which are very small compared to the mean interaction length of primary GCR particles. A reasonable limit might be a pre-atmospheric radius of 5 gram/cm^2, or 1.5 cm for chondrites. These are interesting for at least three reasons: (1) this is a limiting case for larger objects, and can help us make better models, (2) this size is intermediate between usual meteorites and irradiated grams (spherules), and (3) these are the most likely objects to show SCR effects. We are now engaged in a search for suitable objects for experimental study.

Reedy (1984) has recently proposed a model for production by GCR of radioactive and stable nuclides in spherical meteorites. We expect the very small objects to deviate from this model in the direction of fewer secondary particles (larger spectral shape parameter α), at all depths. The net effect will be significantly lower production of such low-energy products as ^{53}Mn and ^{26}Al. The SCR production of these and other nuclides will be lower, too, because meteorite orbits extend typically out into the asteroid belt, and the mean SCR flux must fall off approximately as r^{-2} with distance from the sun. Kepler's laws insure that for such orbits most of the exposure time is spent near aphelion.

None the less the "equivalent mean exposure distance" R_{exp}, is slightly less than the semimajor axis A, in fact $A(1 - e^2)^{1/4}$, because of the weighting by R^{-2}. For the three meteorite orbits we have, R_{exp} has a narrow range, from about 1.6 to 2.1 a.u. This is probably true for the great majority of meteorites. If we take 1.8 a.u. as representative, the SCR flux is lowered by a factor of 3.24.

For a very small meteorite, we can estimate that ^{26}Al produced by GCR is perhaps 30 dpm/kg, while the SCR production will add another 30-40 dpm/kg, with no ablation. Obviously such objects are unlikely to be identified by non-destructive counting. The rarity of high ^{26}Al values is to be expected.

Reference:

Reedy, R. C., Proc. 15th, LPSC (in press).

SIMULATION EXPERIMENTS FOR GAMMA-RAY MAPPING OF PLANETARY SURFACES: SCATTERING OF HIGH-ENERGY NEUTRONS. J. Brückner[1], P. Englert[2], R. C. Reedy[3], and H. Wänke[1]. ([1]Max-Planck-Institut für Chemie, Mainz, FRG; [2]Institut für Kernchemie, Köln, FRG; [3]Los Alamos National Laboratory, Los Alamos, NM, USA)

The concentration and distribution of certain elements in surface layers of planetary objects specify constraints on models of their origin and evolution. This information can be obtained by means of remote sensing gamma-ray spectroscopy (1), as planned for a number of future space missions, i.e. Mars, Moon, asteroids, and comets.

The surface of a planetary body is bombarded by energetic particles of cosmic-rays, which produce a cascade of secondary particles, such as neutrons. Nonelastic scattering and capture reactions of these neutrons play an important role in the production of discrete-energy gamma-ray lines which can be measured by a gamma-ray detector on board of an orbiter. This allows to determine the abundances of many elements, as O, Al, Si, K, Ca, Fe, Th, and U, in the upper 50 centimeters of a planet's surface layer.

To investigate the gamma-rays made by interactions of neutrons with matter, thin targets of different composition were placed between a neutron-source and a high-resolution germanium spectrometer. Gamma-rays in the range of 0.1 to 8 MeV were accumulated.

In one set of experiments (2) a 14-MeV neutron generator using the T(d,n) reaction as neutron-source was placed in a small room. Scattering in surrounding walls produced a spectrum of neutron energies from 14 MeV down to thermal. This complex neutron-source induced mainly neutron-capture lines and only a few scattering lines. As a result of the set-up, there was a considerable background of discrete lines from surrounding material. A similar situation exists under planetary exploration conditions: gamma-rays are induced in the planetary surface as well as in the spacecraft.

To investigate the contribution of neutrons with higher energies, an experiment for the measurement of prompt gamma radiation was set up at the end of a beam-line of the isochronous cyclotron of the KFA Jülich, FRG (cf. fig. 1). Energetic neutrons were produced by bombardement of a 1 cm thick

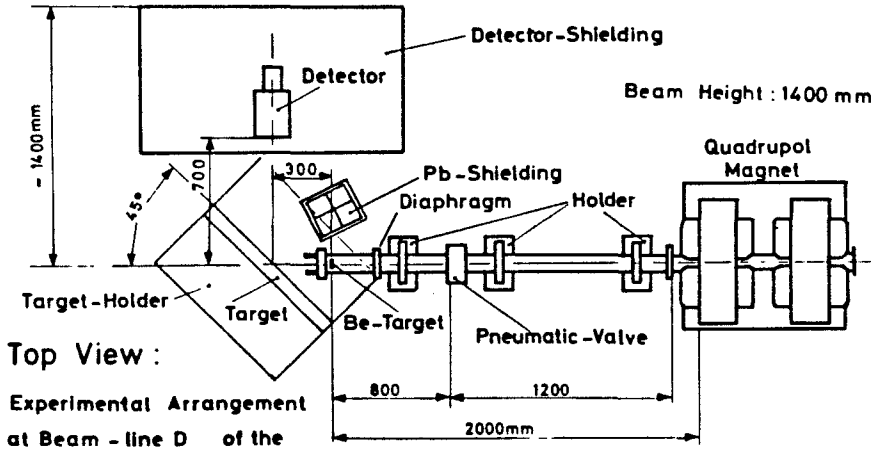

Fig. 1

Be-target with deuterons of energies of 45, 60, and 78 MeV, resulting in maximal neutron energies of 22.5, 30, and 39 MeV respectively. Typical deuteron-beam currents varied between 200 and 600 pA depending on the target material exposed to them. The majority of the neutrons produced by the Be(d,n) reaction is emitted in forward direction and hits the extended targets positioned at an angle of 45° to the beam axis.

Gamma-rays were measured with a 92-cm^3 high purity germanium-detector located at an angle of 90° to the beam axis and 70 cm away from the geometric center of the target-plates. The front side of the detector was shielded by a 2 cm plate made of borated polyethylene. The other sides were consecutively surrounded by lead, boron, and paraffin in order to shield it from background gamma radiation and scattered neutrons. Gamma radiation from the Be-target and its direct environment was suppressed by an additional 20-cm lead shield.

During in-beam operation, the germanium-detector had a resolution of about 6 keV at 7 MeV. The detector signals were processed by conventional amplifiers and ADCs, and stored in 8000 channels of two combined multichannel analyzers.

The gamma-ray spectra were unfolded by an interactive computer program using a modified Gauss-Newton algorithm. A large gamma-ray library provided data for the identification of the source-reactions.

Several correction factors had to be applied to the measured line intensities: i) the total neutron-flux factor was determined by using peaks of suitable reactions in the spectrum itself; ii) the background correction was determined by comparing the gamma-ray emission of targets of different composition; iii) the absolute efficiency was determined by using radioactive standards for the low energy range and by an iron-target for the high-energy range; iv) the mass attenuation coefficient of the detector shielding-material was determined experimentally and the energy dependent absorption factor of the gamma-rays was calculated; v) the gamma selfabsorption factor of the three-dimensional target was calculated by using the appropriate mass attenuation coefficients.

Several targets were irradiated with neutrons of different energies. In contrast to the 14-MeV experiments, the capture lines are very week and result mainly from the surrounding material. The scattering and (n,2n) reaction gamma-rays dominate the spectra (cf. Fe-spectrum in fig. 2).

The gamma-ray lines of e.g. iron and their measured intensities, considering all necessary corrections, are listed in table 1. It can be seen, that the intensities for 30 and 39-MeV neutrons are very similar in most cases. For 22.5-MeV neutrons increased intensities are found for almost all energies. This is a result of the general decrease of the cross sections with increasing energy in the energy interval under question. Compared to 14-MeV, four more lines were observed in the 22.5 and 30-MeV experiments: 1038, 2113, 2523, and 3601 keV. 39-MeV neutrons revealed an additional scattering line at 2601 keV.

Combining the results of the 14-MeV and the 'high-energy' experiments we get a rather realistic simulation of the expected gamma-flux from planetary surfaces. The complexity of the accumulated gamma-ray spectra illustrates what a gamma-ray experiment may encounter during a mission.

Ref.: (1) R. C. Reedy (1978) Proc. Lunar Planet. Sci. Conf. 9th, p. 2961
(2) J. Brückner, R. C. Reedy, and H. Wänke (1984) Lunar Plan. Sci. XV, p.98

GAMMA-ENERGY [keV]	SOURCE-REACTION	NEUTRON ENERGY 22.5 MeV	30 MeV	39 MeV
846.7	Fe(n,ng)	$1.51 \cdot 10^{8}$	$9.65 \cdot 10^{7}$	$9.81 \cdot 10^{7}$
931.2	Fe(n,2ng)	$9.17 \cdot 10^{6}$	$9.43 \cdot 10^{6}$	$1.01 \cdot 10^{7}$
1038.0	Fe(n,ng)	$8.17 \cdot 10^{6}$	$6.78 \cdot 10^{6}$	$6.82 \cdot 10^{6}$
1238.3	Fe(n,ng)	$3.36 \cdot 10^{7}$	$2.42 \cdot 10^{7}$	$2.33 \cdot 10^{7}$
1316.4	Fe(n,2ng)	$7.05 \cdot 10^{6}$	$8.56 \cdot 10^{6}$	$9.11 \cdot 10^{6}$
1407.7	Fe(n,ng)	$7.77 \cdot 10^{6}$	$8.33 \cdot 10^{6}$	$1.16 \cdot 10^{7}$
1810.9	Fe(n,ng)	$1.83 \cdot 10^{7}$	$9.23 \cdot 10^{6}$	$1.01 \cdot 10^{7}$
2112.9	Fe(n,ng)	$9.60 \cdot 10^{6}$	$4.02 \cdot 10^{6}$	$4.41 \cdot 10^{6}$
2523.1	Fe(n,ng)	$4.39 \cdot 10^{6}$	$2.62 \cdot 10^{6}$	$2.80 \cdot 10^{6}$
2601.0	Fe(n,ng)	n.d.	n.d.	$7.28 \cdot 10^{5}$
3601.9	Fe(n,ng)	$9.69 \cdot 10^{5}$	$2.20 \cdot 10^{6}$	$1.45 \cdot 10^{6}$

Table 1. Measured and corrected intensities [dpm] of iron gamma-rays for different neutron energies (n.d. = not determined).

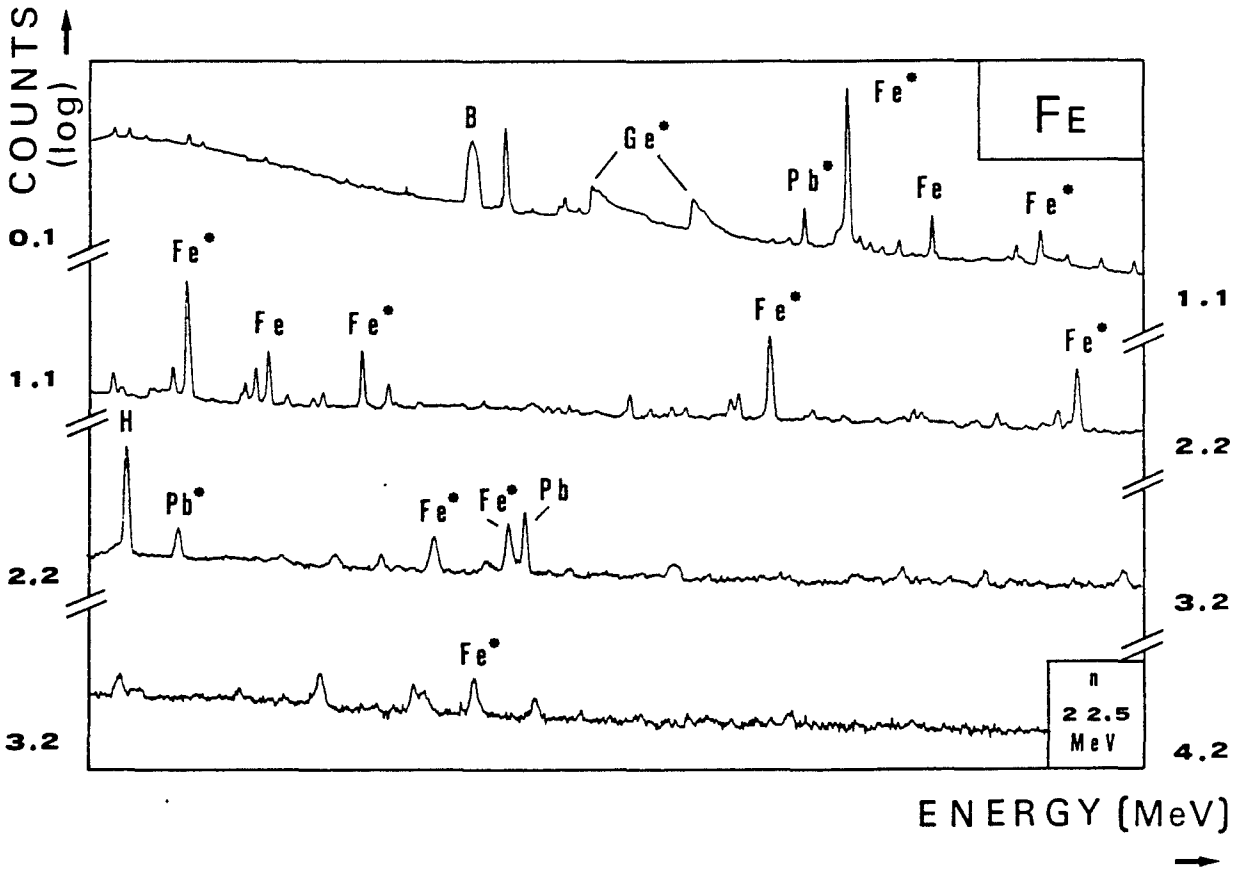

Fig. 2 Low energy part of in-beam gamma-ray spectrum of iron and surrounding material, induced by 22.5 MeV neutrons (* = (n,nγ)).

PRECOMPACTION IRRADIATION EFFECTS: PARTICLES FROM AN EARLY ACTIVE SUN? M. W. Caffee[1], J. N. Goswami[2], C. M. Hohenberg[1], and T. D. Swindle[1]. [1]McDonnell Center for the Space Sciences, Washington University, St. Louis, MO 63130. [2]Physical Research Laboratory, Ahmedabad, India.

Two recent studies have shown that solar flare irradiated grains from Murchison and Kapoeta have excess spallogenic ^{21}Ne compared to unirradiated grains, indicating large precompaction particle irradiation effects. The quantity of cosmogenic neon in these grains presents serious difficulties for either galactic cosmic ray or normal solar flare sources. In the first study it was suggested that the effect might be the result of exposure to an early active sun [1]. The more recent experiment both confirms the earlier results and provides constraints on the characteristic energy spectrum of the irradiation [2].

The first results were obtained from Murchison olivines and Kapoeta pyroxenes by mass spectrometric analysis of sets of grains selected on the basis of the presence or absence of solar flare particle tracks. In the second work plagioclase feldspar grains from Kapoeta were studied, in addition to more olivine grains from Murchison. The feldspars were chosen because the cosmogenic $^{21}Ne/^{22}Ne$ ratio expected from lower energy (present day) solar flare irradiation is about .5, compared to about .8 for the cosmogenic neon produced by the more energetic particles found in galactic cosmic rays [3, 4].

As in the earlier experiment, large precompaction exposure effects were observed. The feldspars show a substantial abundance of cosmogenic neon from high energy particle irradiatons, with measured isotopic compositions populating a mixing line between a trapped (solar-type) endmember and a cosmogenic endmember similar in composition to GCR-produced neon (see figure). For both Kapoeta and Murchison the irradiated grains contain at least an order of magnitude more cosmogenic neon than their unirradiated counterparts. This enrichment is somewhat smaller than that observed in the previous study and may reflect statistical variations in precompaction irradiation effects among individual grains.

The size of the effect in the first study precludes easy explanation in terms of precompaction exposure to galactic cosmic rays, since grains from both meteorites have two orders of magnitude more cosmogenic neon than predicted by most models for the formation of gas-rich meteorites. Little solar wind neon was detected. If the effects are due to galactic cosmic ray exposure, then either the flux of galactic cosmic rays was anomalously high (by at least two orders of magnitude), or models for the formation of gas-rich meteorites have seriously underestimated the duration of exposure of individual grains to cosmic rays.

Solar cosmic rays have even more difficulty. An SCR origin requires a similarly long pre-compaction exposure time (in excess of 100 m.y. at 3 A.U. under present conditions [1]). In addition, the observed isotopic composition of the cosmogenic neon suggests production by more energetic particles and solar wind effects are small. These observations led to the suggestion that pre-compaction irradiation effects may have been due to an early active sun. The most recent results better constrain the energy spectrum of the nuclear-active particles. If the effects are indeed due to an energetic primitive sun, it must have had both a higher flux and a harder energy spectrum than is currently observed.

[1] Caffee, M.W., et al. (1983) Cosmogenic neon from precompaction irradiation of Kapoeta and Murchison. Proc. Lunar Planet. Sci. Conf. 14th, in J. Geo-

phys. Res., 88, B267-B273.
[2] Caffee, M.W., et al. (1984) Confirmation of cosmogenic neon from precompaction irradiation of Kapoeta and Murchison (abstract). In Papers Presented to the 47th Meteoritical Society Meeting, Albuquerque.
[3] Hohenberg, C.M., et al., (1978) Comparisons between observed and predicted cosmogenic noble gases in lunar samples. Proc. Lunar Planet. Sci. Conf. 9th, 2311-2344.
[4] Walton, J.R., et al. (1974) Evidence for solar cosmic ray proton produced neon in fines 67701 from the rim of North Ray Crater. Proc. Lunar Sci. Conf. 5th, 2045-2060.

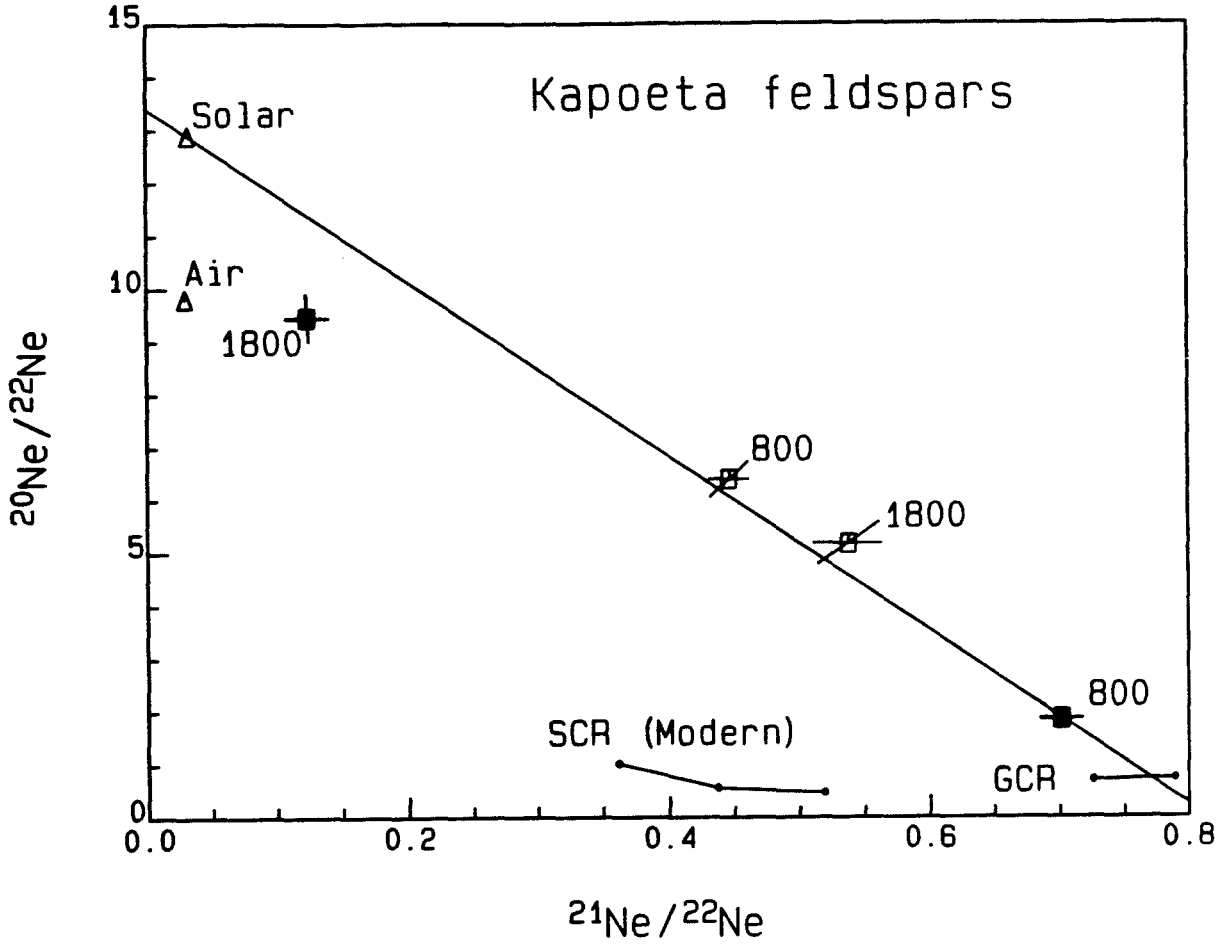

Figure caption: Neon from selected Kapoeta feldspar grains. Closed symbols are solar-flare irradiated grains (identified by the presence of heavy ion tracks), open symbols are grains which do not show solar flare irradiation effects. Numbers represent extraction temperatures in degrees Celsius. Line marked 'GCR' gives range of compositions expected for galactic cosmic ray spallation on targets with the chemistry of the Kapoeta feldspars with shielding of 0 to 40 g/cm². Curve marked 'SCR (Modern)' gives expected compositions from solar cosmic ray irradiation under present solar conditions for shielding depths of 0 to 10 g/cm². Predicted spectra computed from [3].

DETERMINATION OF CA-41, I-129 AND OS-187 IN THE ROCHESTER TANDEM ACCELERATOR AND SOME APPLICATIONS OF THESE ISOTOPES; U.Fehn, D.Elmore, H.E.Gove, P.Kubik, R.Teng, L.Tubbs, G.R.Holdren Nuclear Structure Research Lab., University of Rochester, Rochester, NY 14627

The TAMS program at the University of Rochester was started about seven years ago at the MP Van de Graaff accelerator (nominal voltage 12 MV). At present we measure several hundred samples per year using roughly a third of the accelerator's up-time. Most of the work is concerned with the determination of long-lived, cosmogenic radioisotopes such as Be-10, C-14 and Cl-36. Examples of investigations recently completed or still in progress are the determination of Be-10 in lake sediments in New York [1], the measurement of C-14 in prehistoric vegetables in North America [2] and the investigation of Cl-36 in meteorites [3]. Two more isotopes were added to this list recently, Ca-41 and I-129, the measurement of which will be the focus of this paper. In addition, we will report on our plans to use the $^{187}Os/^{186}Os$ ratio for the differentiation of extraterrestrial material in a meteor crater in Germany.

Calcium-41 has a half-life of 100,000 yrs and is produced in the top few meters of the earth's crust by the interaction of secondary cosmic ray neutrons with Ca-40. After it is released because of weathering it enters the hydrologic cycle and the biosphere. It is thus of potential use for the dating of groundwater as well as of bones in the age range between 50,000 and 1 million years. The expected equilibrium concentrations $^{41}Ca/Ca$ are about 10^{-14} [4], which make detection limits of 10^{-15} necessary for these applications.

A major problem for the measurement of Ca-41 with TAMS is the fact that calcium does not readily form negative atomic ions. It does, however, form negative molecular ions such as CaO^- and CaH_3^-. Another problem is the separation of Ca-41 from its isobar K-41, which is quite common in samples as well as in the cesium of the ion source.

One way to eliminate both of these problems would be to use CaH_3^- because KH_3 apparently does not form negative ions [5]. The probability for formation of CaH_3^- is, however, very low unless calcium metal samples are used. Since the reduction of calcium from small natural samples is quite inefficient and difficult we investigated a different approach, namely the production of negative ions from oxygen bearing Ca molecules. Natural samples (such as bones where Ca occurs as Calcium phosphate) can easily be transformed into CaO or $CaCO_3$ compounds. We studied the production of CaO^- ions from compounds such as CaO and $CaCO_3$ and from oxygen free Ca molecules which were sprayed with oxygen gas. The best results were obtained from CaO and from $CaCO_3$ samples. KO^- ions are, however, present in contrast to KH_3^- ions. The interference of K-41 ions sets a detection limit of approx. $5x10^{-13}$ for the $^{41}Ca/Ca$ ratio under the present conditions.

This detection limit is not sufficient for the measurement of terrestrial samples. Improved chemical procedures during the preparation of the sample and a reduction of the potassium content in the cesium of the ion source will help to lower this detection limit. In addition, we plan to install a new high intensity ion source [6] which should result in a significantly higher ionization rate for the Ca-41 in the samples.

Iodine-129 has several characteristics which are outstanding among the cosmogenic radioisotopes, among them its relatively long half-life of 16 m.y. In nature it has two sources: It is produced in the atmosphere by the interaction of cosmic rays with xenon, and in the crust as daughter product of the spontaneous fission of long-lived radioisotopes, mainly U-238. In addition, a significant amount comes from nuclear bomb tests in the atmosphere.

Because of its low natural concentration relatively few data are available concerning production rates and equilibrium values in the various natural reservoirs. The steady-state ratio of $^{129}I/I$ in the hydrosphere is estimated to be between $3x10^{-13}$ and $3x10^{-12}$ [7,8]. I-129 in this reservoir is derived probably in equal parts from the production in the lithosphere and in the atmosphere [7,9].

These ratios are approx. one order of magnitude higher than the detection limit presently reached with TAMS [10]. A recent measurement of $^{129}I/I$ in the Great Artesian Basin in Australia gave values of $5.7x10^{-13}$ [11] which is in good agreement with the predicted prebomb equilibrium values in the atmosphere. The recent installation of a new injector system will lower the detection limit for I-129 by about one order of magnitude.

A major project we are about to start is the application of I-129 as tracer for hydrothermal convection in sediment-covered oceanic crust. For quite a while now it has been postulated that during the cooling of newly formed oceanic crust seawater penetrates the crust. The reactions occurring between basalt and seawater during this convection change drastically the composition of the circulating fluids and thus may be of great consequence for the element budget of the oceans. Although the most vigorous form of this process occurs right at the active spreading centers, heat flow investigations show that this process is widespread also in older oceanic crust. Because the movement in sediments and older crust is very slow a highly sensitive tracer is needed for the detection of this movement. We plan to use I-129 profiles in conjunction with heat flow measurements in order to determine rate, continuity and extent of this convection in older crust. As a preliminary step of this investigation we are in the process of determining the I-129 content in deep sea sediments from piston cores taken off Cape Hatteras.

Osmium and rhenium are both significantly but not to the same extent depleted in crustal material as compared to extraterrestrial material. This observation combined with the fact that Re-187 is radioactive and decays into Os-187 has led to the suggestion to use the isotopic distribution of osmium as tracer for extraterrestrial material. The Cretaceous-Tertiary boundary is a well publicized example of such an application [12].

We plan to use this approach for the Ries crater in Germany. Although the meteoric origin of this crater has been widely accepted by now it has not been possible so far to identify material of definite extraterrestrial origin. One major obstacle is the dilution of the meteoric material which is significantly higher in the Ries crater than the dilution estimated for the C-T boundary. Calculations of the expected differences in the isotopic composition of Os in the various rock units show, however, that they should be of sufficient magnitude in order to be detectable with TAMS. At present we are in the process of establishing the sensitivity of the accelerator for this isotope system by measuring the Os ratios in artificial samples and in meteorites.

REFERENCES

[1] Wahlen M., Kothari B., Mitchell J., Schwenker C., Elmore D., Tubbs L., Ma X., Gove H.E. (1983) UR-NSRL-267.

[2] Conard N., Asch D.L., Asch N.B., Elmore D., Gove H.E., Rubin M., Brown J.A., Wiant M.D., Farnsworth K.B., Cook T.G. (1984) Nature 308, 443-446.

[3] Nishiizumi K., Arnold J.R., Elmore D., Ma X., Newman D., Gove H.E. (1983) Earth Planet.Sci.Lett. 62, 407

[4] Raisbeck G.M. and Yiou F. (1979) Nature 277, 42

[5] Raisbeck G.M., Yiou F., Peghaire A., Guillot J., Uzureau J. (1981) Proc. Symp. Accel. Mass Spectr., Argonne Nat. Lab.

[6] Middleton R. (1982) Nucl.Instr.Meth. 214, 139-150.

[7] Fabryka-Martin J. (1984) Ms.Thesis, University of Arizona.

[8] Kohman T.P. and Edwards R.R. (1966) U.S. A.E.C. NYO-3624-1, 41p.

[9] Edwards R.R. and Rey P. (1968) U.S. A.E.C. NYO-3624-3, 30p.

[10] Fabryka-Martin J., Bentley H., Elmore D., Airey P.L. (1984) Geochim. Cosmochim. Acta, submitted.

[11] Elmore D., Gove H.E., Ferraro R., Kilius L.R., Lee H.W., Chang K.H., Beukens R.P., Litherland A.E., Russo C.J., Purser K.H., Murrell M.T., Finkel R.C. (1980) Nature 286 138-140.

[12] Luck J.M. and Turekian K.K. (1983) Science 222, 847.

SOLAR MODULATION OF GALACTIC COSMIC RAYS: CONTEMPORARY OBSERVATIONS AND THEORIES: M. A. Forman, Dept. of Earth and Space Sciences, State University of New York at Stony Brook, NY 11794

The flux of galactic cosmic rays inside the solar system is modulated by the action of the complex magnetic fields carried from the sun by the solar wind. This is apparent from the recurrent decrease of about 20% in the intensity of relativistic cosmic rays during sunspot maximum compared to sunspot minimum, from transient decreases due to solar flares and many other subtler effects observed by ground stations for the last 50 years. Spacecraft observations of the spatial and temporal variations of cosmic ray flux during the last ten years have shown that the solar wind and cosmic-ray modulation extend to at least 30 astronomical units in the ecliptic plane. Present best guesses are that it goes out to 100 or 200 AU, perhaps less over the poles.

Understanding the mechanism and detailed effect of modulation on the intensity, energy and composition of galactic cosmic rays is important for three reasons:

For interpreting cosmogenic nuclide fluctuations, we need to know what solar parameters control their production rates in order to know what aspect of solar variability they measure; and we need to predict production rate fluctuations from known solar parameters, to find the geophysical component of variations in cosmogenic nuclide concentration.

For galactic astrophysics, to understand the origin of cosmic rays in the galaxy, we need to know how to remove the modulation effect from the data. We need to find the spectrum of each element and isotope, including exotic species such as helium-3 and anti-protons far outside the solar system from the measurements we can make inside it.

For high energy plasma astrophysics, cosmic-ray behavior in the solar wind is a locally observable phenomenon which suggests and tests theories later applied to solar flares, x-ray stars, pulsars, quasars and other objects where energetic particles and supersonic turbulent plasma flows have been inferred.

The mechanism of solar modulation is understood in part, but how the parts act together to make the whole effect is still controversial. Parker's (1958) original concept of modulation by diffusion and convection in the solar wind remains the basis for all current descriptions. Until a few years ago, the "force-field"approximation seemed to be adequate, at least for relativistic particles. It included all the important physics of modulation and described the observations reasonably well. "Force-field" will be described in the talk, but the conditions of its validity and meaningfulness will be made clear.

Observations in the outer heliosphere show that there is a positive radial gradient of 3% per astronomical unit in the ecliptic plane. In addition, abrupt decreases occur behind certain flare-initiated shock structures. These structures, and the modulation behind them propagate outward with the solar wind. One view is that the steady gradient is always present, due to local diffusion, but that the variation during the solar cycle is due simply to the increase in the number of these regions of abrupt decrease in the heliosphere at solar maximum.

At the same time, observations of the heliospheric magnetic field near solar minimum a little off the ecliptic plane showed a very large-scale coherent structure. Field is directed outward in the northern solar hemisphere, and inward in the south, with a warped and wavy neutral sheet between these huge volumes.

Theoretically, this magnetic geometry forces galactic cosmic rays to "drift" down from the poles and out through the neutral sheet. The flow of energetic particles is reversed in the next solar minimum. The wavy character of the neutral sheet and the changing source region makes successive solar minima different-as they seem to be in the cosmic ray flux. The drift mechanism accounts for the amount of modulation at solar minimum only by the strength of the magnetic field. The amount of turbulence and the speed of the solar wind are irrelevant.

Drifts must occur at solar minimum when the fields are smooth, but are not necessarily important at solar maximum when the field is choppy and changing. On the other hand, drifts provide the least level of solar modulation. These must have disappeared during the Maunder and earlier minima in the radiocarbon record. This would imply that the solar magnetic field was very weak, but not that the solar wind was weak or absent. Drift effects are strongly three-dimensional poleward of the wavy neutral sheet. It is hoped that the single spacecraft mission over the solar poles in the late 1980's will resolve the question of the role of drifts in the solar modulation of galactic cosmic rays.

EVOLUTION OF GAS-RICH METEORITES : CLUES FROM COSMOGENIC NUCLIDES, J.N. Goswami, Physical Research Laboratory, Ahmedabad 380 009, India.

The evolution of gas-rich meteorites in general, and the setting in which the observed solar-wind, solar-flare irradiation records were imprinted in individual components of these meteorites are understood only in qualitative terms, although contrary viewpoints do exist (Goswami et al. 1984 and references therein). The regolith irradiation hypothesis, bolstered by the observations of irradiation features in lunar regolith materials, similar to those observed in gas-rich meteorites, is accepted by many workers in this field. However, a close analysis of the problem suggests that the regolith irradiation may not be the dominant mode in producing the observed precompaction irradiation features in the gas-rich meteorites.

It is generally assumed that the irradiated and non-irradiated components in the gas-rich meteorites, and particularly in the so-called 'dark-phase' material evolved together. Starting with this assumption, one can use the data on cosmogenic nuclides in gas-rich meteorites to impose strong constraints on the maximum residence time for the individual components of these meteorites within the nuclear active zone (approximately the upper meter) of the asteroidal regolith. This turns out to be $\lesssim 10^5$ years in the case of CI and CM chondrites and $\lesssim 10^6$ years for H-chondrites and achondrites (Goswami and Lal 1979; Goswami and Nishiizumi 1982; Goswami et al 1984; Goswami and Nishiizumi 1984). These values were obtained by considering the difference between the cosmogenic noble gas (^{21}Ne; ^{38}Ar) and radionuclide (^{26}Al; ^{53}Mn) exposure ages of these meteorites. Such an approach is valid as the precompaction irradiation of gas-rich meteorites must have taken place during their early evolutionary history. Although the short precompaction exposure durations for gas-rich meteorites was noted earlier by Anders (1975), this constraint was never considered explicitely in treating the problem of evolution of these meteorites. The implications of a very short ($\lesssim 10^5$ years) precompaction exposure duration in the case of carbonaceous chondrites have been discussed in detail by Goswami and Lal (1979), Goswami and Macdougall (1983) and Goswami et al. (1984), which clearly show the incompatibility of the regolith irradiation scenario for these meteorites given our present understanding of asteroidal regolith dynamics (Housen et al. 1979; Langevin and Maurette 1980; Housen and Wilkening 1982a). The 'small body' irradiation model was proposed instead (Goswami and Lal 1979; Goswami et al. 1984) in which the irradiation preceds formation of the parent bodies of the carbonaceous chondrites and occur when the individual components of these meteorites were part of cm to meter-sized objects. In the case of gas-rich H-chondrites and achondrites, the time constraint imposed by cosmogenic nuclide data is barely within the limit of the regolith model (Housen and Wilkening

1982b). However consideration of certain specific aspects, e.g. finer details of solar flare irradiation records and petrographic constraint (presence of significant fraction of gas-rich H-chondrites among all petrographic types) suggest that the regolith model may not adequately explain all these observations. Unfortunately only one achondrite (Kapoeta) and a couple of H-chondrites with high solar-wind content have been analysed in detail for their cosmogenic records (Goswami and Nishiizumi 1982; 1984). This is primarily due to the fact that saturation effect in ^{26}Al and ^{53}Mn concentrations constrain the analysis to gas-rich meteorites with exposure age <10 m.y. In this context it will be extremely useful to use the newly developed accelerator mass-spectrometry method of determining cosmogenic ^{129}I (Nishiizumi et al. 1983) to analyse a suite of gas-rich H-chondrites with noble gas exposure age exceeding 10 m.y.,and having high level of solar-wind and solar-flare irradiation. Fayetteville and Elm Creek will be two ideal candidates for such a study.

A new dimension to the problem of evolution of gas-rich meteorites was added by the recent findings of Caffee et al. (1983) that the solar flare irradiated grains in the gas-rich meteorites Kapoeta and Murchison have more than an order of magnitude higher cosmogenic ^{21}Ne in them compared to the concentrations measured in non-irradiated grains from these same meteorites. Whether this can be taken to imply an early active Sun, characterized by a harder solar flare proton spectrum, or is indicative of a very different evolutionary pathway for the irradiated components in gas-rich meteorites could be ascertained only through further work in this direction. In summary, a reappraisal of our understanding of the evolution of gas-rich meteorites is necessary considering the new inputs provided by the records of cosmogenic nuclides in these meteorites.

References: Anders E. (1975) Icarus 24, 363-371; Caffee M.W. et al (1983) J. Geophys, Res. 88, B 267-B 273; Goswami J.N. and Lal D. (1979) Icarus 40, 510-521; Goswami J.N. and Nishiizumi K. (1982), LPI Tech. Rep. 82-02, 44-48; Goswami J.N. and Macdougall J.D. (1983) J. Geophys. Res. 88, A 755-A 764; Goswami J.N. and Nishiizumi K. (1984) In Preparation; Goswami J.N., Lal D. and Wilkening L.L. (1984) Sp. Sci. Rev. 37, 111-159; Housen K. et al. (1979) Icarus 39, 317-351; Housen K. and Wilkening L.L. (1982a) Ann. Rev. Earth Planet. Sci. 10, 355-376; Housen K. and Wilkening L.L. (1982b) Lunar and Planetary Sci. XIII, 339-340; Langevin Y. and Maurette M. (1980) Lunar and Planetary Sci.XI, 602-604; Nishiizumi K. et al (1983) Nature 305, 611-612.

THE EXPOSURE HISTORY OF JILIN AND PRODUCTION RATES OF COSMOGENIC NUCLIDES; G. Heusser, Max-Planck-Institut f. Kernphysik, POB 103980, D-6900 Heidelberg, Germany

Jilin the largest known stone meteorite is a very suitable object for studying the systematics of cosmic ray-produced nuclides in stony meteorites. Its well established two stage exposure history (1,2,3) even permits to gain information about two different irradiation geometries (2π and 4π).

All stable and long-lived cosmogenic nuclides measured in Jilin so far correlate well with each other (3,4,5). An example is shown in Fig. 1 where the ^{26}Al activities are plotted vs. the spallogenic ^{21}Ne concentration (6,7).

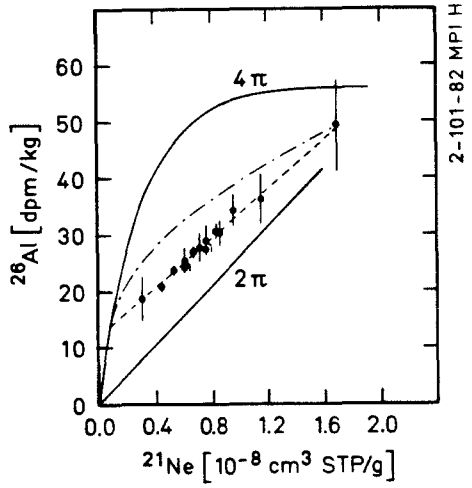

Figure 1: ^{21}Ne-^{26}Al correlation in Jilin and its evolution from a 2π irradiation geometry followed by a 4π irradiation geometry. ^{21}Ne from (6,7).

These records of cosmic-ray interaction in Jilin can be used both to determine the history of the target and to study the nature of production rate profiles. This is unavoidably a bootstrap process, involving studying one with assumption about the other.

The good correlation (dotted line in Fig. 1) with a positive ordinate intercept is interpreted in terms of a 2π irradiation followed by a 4π irradiation.

The production of stable (S) and radioactive (R) nuclides by cosmic rays in a large body (2π geometry) can be described by:

$$S(d) = P_S(d)\ t \qquad (1)$$

$$R(d) = P_R(d)\ (1-e^{-\lambda t}) \qquad (2)$$

where $P_S(d)$ and $P_R(d)$ are the depth-dependent production rates of the stable and radioactive species, respectively and t is the exposure time. Both expressions can be combined:

$$R(d) = \frac{P_R(d)}{P_S(d)} \frac{1-e^{-\lambda t}}{t} S(d) \qquad (3)$$

For a given t and a constant production rate ratio $P_R(d)/P_S(d)$ this is the equation of a straight line R=m·S through the origin (solid line labelled 2π in Fig. 1). Its slope is determined by the production rate ratio and the duration of exposure.

For a 4π irradiation with negligible depth effects for the production of spallogenic nuclides as indicated by the measured ^{22}Na activities in Jilin (3) the production equations

$$R = P_R(1-e^{-\lambda t}) \text{ and } S = P_S t$$

represent the curve of growth in the R vs. S diagram (Fig. 1, labelled 4π)

$$R = P_R(1-e^{-\lambda\frac{S}{P_S}}) \tag{4}$$

If a 2π irradiation is followed by a 4π irradiation, the relevant production rates are expressed by:

$$S(d) = P_{S1}(d)t_1 + P_{S2}t_2 \tag{5}$$

$$R(d) = P_{R1}(d)(1-e^{-\lambda t_1})\, e^{-\lambda t_2} + P_{R2}(1-e^{-\lambda t_2}) \tag{6}$$

where P_1 and P_2 are the production rates of the first (2π) stage and the second (4π) stage, respectively and t_1 and t_2 are the respective exposure ages. Again with the assumption of a constant production ratio we get:

$$R(d) = \frac{P_R(d)}{P_S(d)} \frac{1-e^{-\lambda t_1}}{t_1}\, e^{-\lambda t_2}\, S(d) + \tag{7}$$

$$+ P_{R2}\{1+ \frac{t_2}{t_1} e^{-\lambda t} - \frac{t}{t_1} e^{-\lambda t_2}\} \quad \text{with } t = t_1+t_2$$

For t_1 and t_2 fixed equation 7 is the equation of a straight line of the form $R = mS+b$ with slope

$$m = \frac{P_R(d)}{P_S(d)} \frac{1-e^{-\lambda t_1}}{t_1} e^{-\lambda t_2} \tag{8}$$

As t_2 increases for t fixed, the intercept of the original 2π straight line is shifted upwards along the curve of growth while its slope is decreasing. The fit line through the data points obtained for Jilin (dotted line in Fig.1) illustrates this behaviour. The straight line and the curve of growth intersect at

$$R_{inters.} = P_{R2}(1-e^{-\lambda t_2}) \tag{9}$$

Hence t_2 can be calculated if P_{R2} is known. We can then enter the value of t_2 into equation (8) and obtain t_1 by iteration, provided that we know the production rate ratio. With well founded assumptions about the individual production rates eq. (9) yields t_2=0.4 Myr and eq. (8) t_1=9 Myr (3). If the stable isotope is replaced by a long-lived radionuclide, the general equation of the correlation line has the form:

$$R_A(d) = \frac{R_A}{R_B} \frac{e^{-\lambda_A t_2} - e^{-\lambda_A t}}{e^{-\lambda_B t_2} - e^{-\lambda_B t}} (R_B(d) - P_{A2} + P_{A2} e^{-\lambda_B t_2}) + (1-e^{-\lambda_A t_2})\, P_{A2} \quad \text{with}$$

$t = t_1+t_2$. A is the radionuclide with the shorter half life.

Accepting the nature of Jilin's exposure history, we can now turn to the information provided by these correlations in view of production rate ratios and individual production profiles. The perfect straight line fit of the data points (Fig.1) confirms our assumption of a constant production ratio (eq. 3, 7, and 8), i.e. the production rate of ^{26}Al must have a depth dependence very similar to ^{21}Ne. The sensibility of this behaviour is illustrated as an example for the case that the mean half thickness of ^{21}Ne is twice that of ^{26}Al. The calculation was normalized for the highest data point. The resulting correlation (point-dotted curve in Fig.1) corresponds to a bend curve which is very distinct from the straight line formed by the experimental points. In this way, the depth dependence of production rates of other long-lived and stable cosmogenic nuclides could be investigated in Jilin as well.

References

(1) Honda M., Nishiizumi K., Imamura M., Takaoka M., Nitoh O., Horie K and Komura K. (1982) Earth Planet.Sci.Lett. 57, p. 101

(2) Heusser G., Ouyang Z. (1981) Meteoritics 16, p. 326-327.

(3) Heusser G., Ouyang Z, Kirsten T., Herpers U. and Englert P. (1984) to be published in Earth Planet.Sci.Lett.

(4) Pal D.K., Moniot R.K., Kruse T.H., Tuniz C. and Herzog G.F. (1982) Proc. 5th Int.Conf. Geochronology, Cosmochronology, Isotope Geology, Nikko/ Japan, p. 300 -301.

(5) Osadnik G., Herpers U. and Herr W. (1981) Meteoritics 16, p. 371-372.

(6) Begemann F., Li Z., Schmitt-Strecker S., Weber H.W. and Xu Z. (1984) to be published in Earth Planet.Sci.Lett.

(7) Weber H.W., private communication.

RADIONUCLIDE MEASUREMENTS BY ACCELERATOR MASS SPECTROMETRY AT ARIZONA. A. J. T. Jull, D. J. Donahue, and T. H. Zabel*. NSF Accelerator Facility for Radioisotope Analysis, University of Arizona, Tucson, Arizona 85721. *current address: IBM Thomas J. Watson Research Center, Yorktown Heights, New York 10598.

Over the past few years, Tandem Accelerator Mass Spectrometry (TAMS) has become established as an important method for radionuclide analysis. Measurements of ^{10}Be and ^{14}C are now routine in several laboratories (1). The basic principles of accelerator mass spectrometry have been reviewed by Litherland (2). All systems are basically similar in principle.

In the Arizona system (see fig. 1) we operate the accelerator at a terminal voltage of 1.8MV for ^{14}C analysis, and 1.6 to 2MV for ^{10}Be (3). Samples are inserted into a cesium sputter ion source in solid form. Negative ions sputtered from the target are accelerated to about 25kV, and the injection magnet selects ions of a particular mass. In the case of ^{14}C, N does not produce negative ions and an important source of background is eliminated. The ions are accelerated to the terminal potential of up to 2MV. They then pass through a stripper canal, losing electrons. The resultant positive ions are then accelerated back to ground. Ions of the 3+ charge state, having an energy of about 8MeV are selected by an electrostatic deflector, surviving ions pass through two magnets, where only ions of the desired mass-energy product are selected. The final detector is a combination ionization chamber to measure energy loss (and hence, Z), and a silicon surface-barrier detector which measures residual energy. After counting the trace isotope for a fixed time, the injected ions are switched to the major isotope (^{13}C or ^{9}Be) used for normalisation. These ions are deflected into a Faraday cup after the first high-energy magnet (M1). Repeated measurements of the isotope ratio of both sample and standards results in a measurement of the concentration of the radionuclide.

An important part of TAMS dating is the ability to produce accelerator targets on a consistent and routine basis. For ^{14}C, graphite is the best target because of its high negative ion yield and stability for extended periods of time. Recent improvements in sample preparation for ^{14}C (4) make preparation of high-beam current graphite targets directly from CO_2 feasible. Routine measurements up to now at Arizona have been made on iron-carbon targets, made by dissolution of about 1 mg carbon in 15 mg iron (5). The ^{14}C background using this method is equivalent to approximately 2% modern carbon. This level is almost entirely due to ^{14}C introduced during sample preparation. Lower backgrounds of as low as 0.4% modern carbon ($^{14}C/^{12}C = 4 \times 10^{-15}$) have been measured from carbon produced directly from CO_2/H_2 gas mixtures. If the background level is constant, it can be subtracted, and the detection limit is the error in the background (2 sigma).

Extraction of spallogenic ^{14}C from rocks and meteorites (6) requires temperatures at or near the melting point and oxidising conditions to ensure complete extraction of ^{14}C. By contrast, the chemistry for extraction of ^{10}Be is relatively standardised, the only criterion is to limit contamination by the isobar ^{10}Be.

Except for some measurements of standards and backgrounds for ^{10}Be, our measurements to date have been on ^{14}C. We expect to have more ^{10}Be measurements in the near future. The facility at Arizona has produced a large amount of data on ^{14}C. Although most results have been in archaeology and quaternary geology (3,7), we have expanded our studies to include cosmogenic ^{14}C in meteorites, in collaboration with Fireman (8). The data obtained so far tend to confirm the antiquity of Antarctic meteorites from the Allan Hills site. Data on three samples of Yamato meteorites gave terrestrial ages of between about 3 and 22 thousand years. More samples need to be studied, and comparisons made with other cosmogenic nuclides on the same material, before conclusions as to the terrestrial age distribution of the Yamato collection. The study of samples exposed to simulated cosmic-ray irradiation should also aid in the intercomparison of data on different radionuclides.

References.

1.) Wölfli, W., ed. (1984), Third International Symposium on Accelerator Mass Spectrometry, Zurich. Nuclear Inst. Methods, in press.
2.) Litherland, A. E. (1980), Ann. Rev. Nucl. Part. Phys. 30, 437-473.
3.) Donahue, D. J. et al. (1983), Nucl. Inst. Methods 218, 425-429.
4.) Vogel, J. et al. (1984), Nucl. Inst. Methods, in press.
5.) Jull, A. J. T. et al. (1984), Nucl. Inst. Methods 218, 509-514.
6.) Fireman, E. L. (1979), Proc. Lunar Planet. Sci. Conf. 10th, p. 1053-1060.
7.) Donahue, D. J. et al. (1984), Nucl. Inst. Methods, in press.
8.) Jull, A. J. T. et al. (1984), Proc. Lunar Planet. Sci. Conf. 15th, in press.

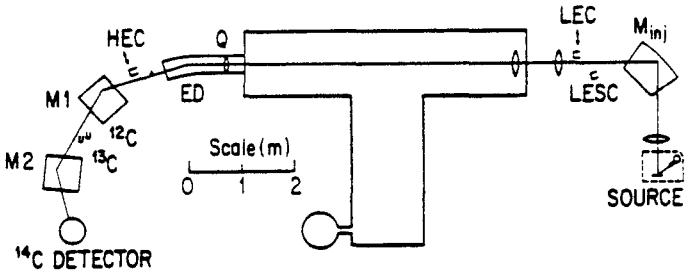

Figure 1. Schematic diagram of system. Abbreviations in the figure are: M_{inj}, injection magnet; LEC, low-energy Faraday cup (this cup can be moved in and out of the beam); LESC, low-energy side cup; Q, electrostatic quadrupole focus; ED, electrostatic deflector; M1 and M2, high-energy magnets, ^{13}C and ^{12}C, high-energy Faraday cups.

COSMIC RAY INTERACTIONS IN THE GROUND: TEMPORAL VARIATIONS IN COSMIC RAY INTENSITIES AND GEOPHYSICAL STUDIES; D. Lal, Scripps Institution of Oceanography, Geological Research Division, A-020, La Jolla, CA 92093 (USA).

Temporal variations in cosmic ray intensity have been deduced from observations of products of interactions of cosmic ray particles in the moon, meteorites, and the earth (1). Of particular interest is a comparison between the information based on earth and that based on other samples. Differences are expected at least due to (i) differences in the extent of cosmic ray modulation, and (ii) changes in the geomagnetic dipole field. Any information on the global changes in the terrestrial cosmic ray intensity is therefore of importance. As an illustration, it is generally believed that the slow variation in $^{14}C/^{12}C$ ratios as observed in tree rings is indicative of an appreciable change in the earth's dipole field during the past 10,000 yrs (2). However, I have recently shown (3), on the basis of theoretical considerations and oceanic paleodata covering the past glaciation, that climate-induced changes in the carbon cycle are large and may be responsible for a greater part of the observed variation. To check on this, one would have to study the temporal variations in the production rate of another terrestrial cosmic ray-produced isotope. One of the obvious ways to achieve this goal is to study the temporal variations in the fallout of an isotope. The potential usefulness of ^{10}Be for this purpose was explored earlier (4) and also recently (5). However, this method presents some difficulties since the fallout of ^{10}Be depends also on meteorological factors (6).

In this paper we present another possibility of detecting changes in cosmic ray intensity. The method involves human intervention and is applicable for the past 10,000 yrs. Studies of changes over longer periods of time are possible if supplementary data on "age" and history of the sample are available using other methods. We also discuss the possibilities of studying certain geophysical processes, e.g. erosion, weathering, tectonic events based on studies of certain cosmic ray-produced isotopes for the past several million years.

(a) Cosmic ray intensity studies. A direct method of measuring cosmic ray intensity on the earth will be to measure the activation products in a sample exposed to the secondary cosmic ray beam for a known period of time, in a known geometry at atmospheric depth, x ($gm \cdot cm^{-2}$) and geomagnetic latitude, λ. At great depths in the atmosphere, the nucleonic component attenuates with a mean free path of 165 $gm \cdot cm^{-2}$. Consequently, samples which are buried underground at depths exceeding 10 m.f.p. (5-6 meters of typical surface materials) will be appreciably shielding so that the unshielded production over periods of the order of (10^3-10^4) yrs will considerably exceed the earlier production. The in-situ production of ^{10}Be, ^{26}Al, ^{36}Cl, ^{3}H and other isotopes can be conveniently measured in rocks exposed for periods of the order of 10^3 yrs, in samples of the order of 100 grams. This is based on production rates given earlier (6).

We therefore propose that changes in the cosmic ray intensity can be directly measured from a study of in-situ production of radionuclides in documented samples. A number of possibilities arise; one of the obvious possibilities is to study the pyramidal stones. The pyramids at Dahsur and Giza seem ideal for providing samples exposed for (4500-4600) yrs. The low latitude of the pyramids is favorable for studying decreases in geomagnetic

dipole field. Tree rings may also serve as ideal in-situ materials for isotope ^{10}Be in particular. Of course, it would have to be ascertained that no appreciable contributions arise from ^{10}Be in ground waters. Geological specimens, e.g. volcanics may well provide ideal samples exposed in fixed geometry for longer periods of time, (10^4-10^5) yrs.

The in-situ method proposed above was considered earlier (7) for the study of long term variations in the flux of high energy primary cosmic rays (E >130 GeV). The present proposal for studying variations in the low energy flux of cosmic rays, in the GeV region which is sensitive to changes in the earth's dipole field, is being made for the first time. This would supplement any information based on the fall-out of nuclides, such as that based on ^{10}Be in polar ice (5).

(b) Geophysical studies. Considering the present detection limits for several isotopes, in the range of 10^5-10^6 atoms (8), one can investigate production rates of $\gtrsim 10^{-11}$ atoms/g·sec in a sample of 1 Kg exposed for a period of 10^6 yrs.

At sea level, the nuclear reactions are produced primarily by neutrons and negative mu-mesons (6). At depths exceeding 2-3 meter rock equivalent, fast mu-mesons and slow negative mu-mesons (captures by nuclei) produce most of the nuclear reactions; neutrons are not important at these depths. Fast mu-mesons produce nuclear disintegrations with larger kinetic energy dissipation in the spallation products than in the case of capture of negative mu-mesons. The nuclear disintegration rate at a depth of say 25 meters rock equivalent is about 2×10^{-9}/gm·sec (6, 7). Compared to sea level, this is lower by a factor of 10^4, but nevertheless such disintegration rates can be monitored using present day atom detection methods.

The main aim of the study (9, 10, 11) would be to measure departures from equilibrium concentrations and then determine the rates of geophysical processes responsible using certain models. If, for example, a sample of rock exposed to elements is continually undergoing weathering, the in-situ cosmic ray production rate of isotopes at a test point will change in view of the reduction in the overlying amount of rock. Let Q(t) be the rate of production. The concentration of a radionuclide in the rock, C(T), after an elapse of time T will then be given by the convolution integral

$$C(T) = C(0)\, e^{-\lambda T} + \int_0^T Q(t)\, e^{-\lambda(T-t)}\, dt \qquad (1)$$

where λ is the disintegration constant of the nuclide and C(0) is the concentration of the nuclide at t = 0. If one isotope is measured, equation (1) can put some constraints in the temporal changes in the rock geometry due to physical processes. It is clearly advantageous to study as many isotopes as possible and also call on supplementary geophysical evidence to model the isotope production with changing geometry of irradiation, due to geophysical processes.

The crux of application of in-situ production of cosmic ray nuclides to geophysical studies lies in equation (1) and the capabilities to model Q(t) in a realistic manner. If this can be achieved, a number of applications should become possible:

i) Rates of erosion of exposed rocks and problems of similar nature involving changes in rock geometry (fragmentation of rocks, sediment burial/denudation, etc.).
ii) Tectonic uplift or subduction.
iii) Residence time of materials in particular settings, e.g. ages of glaciers, and turn-over time of sand dunes.

We will present worked out examples to support the above suggestions, and indicate the type of information which is possible with the isotopes which can currently be detected with high sensitivity. Reference is made to the first application of the method by Hampel et al. (10) to study rock erosion rates, and to a paper by Jha and Lal (11) who have specifically considered the application of ^{10}Be and ^{26}Al to the study of tectonic movements. These isotopes should allow convenient study of vertical movements in the range $(10^{-4}-10^{-5})$ $cm \cdot yr^{-1}$.

REFERENCES

1. Reedy et al., 1983. Ann. Rev. Nucl. Part. Sci. 33, 505-37.
2. Bucha, V., 1970. In 'Radiocarbon Variations and Absolute Chronology,' ed. I. U. Olsson, John Wiley & Sons, 501-11.
3. Lal, D., 1984. To appear in Proc. AGU Chapman Conf. on 'Carbon Cycle Variations During the past 50,000 Yrs,' Tarpon Springs; USA; Lal, D. and R. Revelle, 1984. Nature 308, 344-46.
4. Harrison, C. G. A. and B. L. K. Somayajulu, 1966. Nature 212, 1193-95.
5. Beer et al., 1984. In Proc. 3rd Int. Symp. on AMS, Zurich, 1984, Nucl. Instr. & Methods (in press).
6. Lal, D. and B. Peters, 1967. Handbuch der Physik (Springer-Verlag, Berlin), XLVI/2, 551-612.
7. Lal, D., 1963. Proc. Int. Cosmic Ray Conf. 6th, 190.
8. Rucklidge et al., 1981. Nucl. Inst. & Methods 191, 1-9.
9. Davis, Jr., R. and O. A. Schaeffer, 1955. Ann. N. Y. Acad. Sci. 62, 105.
10. Hampel et al., 1975. Jour. Geophys. Res. 80, 3757-60.
11. Jha, R. and D. Lal, 1982. In 'Proc. 2nd Symp. on Natural Radiation Environment,' eds. K. G. Vohra, et al. Wiley Eastern, New Delhi, 629-35.

PRODUCTION RATES OF NEON AND XENON ISOTOPES BY ENERGETIC NEUTRONS

D. A. Leich, R. J. Borg, and V. B. Lanier, Lawrence Livermore National Laboratory, Livermore, CA 94550

As a first step in a new experimental program to study the behavior of noble gases produced in situ in minerals, we have irradiated a suite of minerals and pure chemicals with 14.5 MeV neutrons at LLNL's Rotating Target Neutron Source (RTNS-II) and determined production rates for noble gases. While neutron effects in meteorites and lunar samples are dominated by low-energy (<1 keV) neutron capture, more energetic cosmic-ray secondary neutrons can provide significant depth-dependent contributions to production of cosmogenic nuclides through endothermic reactions such as (n,2n), (n,np), (n,d) and (n,alpha). Production rates for nuclides produced by cosmic-ray secondary neutrons are therefore useful in interpreting shielding histories from the relative abundances of cosmogenic nuclides.

Samples were vacuum encapsulated in quartz ampoules and irradiated as add-ons to the principle RTNS-II experiments for two to four weeks, during which time they accumulated fluences up to 10^{17} neutrons/cm^2 as determined by activation of iron dosimetry foils. Irradiated samples were stored for at least three months before breaking open the quartz ampoules and weighing portions for analysis. Noble gas isotope dilution analyses were performed by adding an aliquot of our mixed noble gas spike (principally ^{3}He, ^{21}Ne, ^{38}Ar, ^{80}Kr, and ^{124}Xe) or of an air standard during a single 1650 C vacuum extraction. Duplicate samples were analyzed without the spike in two-step extractions: a 400 C heating to reveal any tendency for low-temperature gas loss, and a 1650 C extraction. Only insignificant quantities of noble gas reaction products were released in the 400 C steps, leading us to conclude that gas retention was probably quantitative, although we cannot rule out the possibility of some recoil loss during the irradiations or diffusive loss at ambient temperatures during and after the irradiations.

Neon analyses were performed on samples of sodium and magnesium minerals and reagents. The neon extracted from sodalite, albite, and NaCl samples are isotopically similar, determining the composition of Na-derived neon as ^{20}Ne:^{21}Ne:^{22}Ne = 0.45:0.017:1, not including the ^{22}Ne that will grow in from decay of 2.6-year ^{22}Na from ^{23}Na(n,2n)^{22}Na. The neon extracted from the magnesium minerals enstatite and forsterite are also isotopically similar, with a composition given by ^{20}Ne:^{21}Ne:^{22}Ne = 0.61:1:0.090 attributed to

production from natural magnesium. The neon extracted from Mg metal was isotopically different from the neon extracted from the magnesium minerals, probably due partly to differences in the neutron energy spectrum seen by the different samples and partly to atmospheric neon contamination in the Mg metal. Unlike the other reagent samples, it had not been degassed by vacuum melting before encapsulation. At present, we can only give the measured isotopic composition in the unspiked 1650 C extraction from this sample as limits for the Mg-derived neon: $^{20}Ne/^{21}Ne < 0.75$, $^{22}Ne/^{21}Ne < 0.095$. The atmospheric neon contamination does not compromise the isotope dilution analysis of ^{21}Ne production in Mg-metal, and our value of 136 $\pm$ 7 mb for this production cross section is in fair agreement with previous measurements of 160 $\pm$ 8 mb at 14.1 Mev and 152 $\pm$ 12 mb at 14.7 MeV (1).

Xenon analyses were performed on samples of CsCl and $Ba(NO_3)_2$. The Cs-derived xenon was dominated by ^{132}Xe primarily from $^{133}Cs(n,2n)^{132}Cs$, but ^{130}Xe from $^{133}Cs(n,alpha)^{130}I$ was also measured, with $^{130}Xe/^{132}Xe = 0.0014$. The major isotopes in the Ba-derived xenon were ^{131}Xe from $^{132}Ba(n,2n)^{131}Ba$ and ^{129}Xe from $^{130}Ba(n,2n)^{129}Ba$. Lesser amounts of other xenon isotopes were also produced, with relative abundances given by $^{129}Xe:^{130}Xe:^{131}Xe:^{132}Xe:^{134}Xe = 1:0.019:1.084:0.221:0.194$.

Absolute production cross sections were calculated from the isotope dilution analyses of the NaCl, Mg, CsCl, and $Ba(NO_3)_2$ samples, assuming purity, stoichiometry, and quantitative noble gas retention and extraction. Relative production cross sections determined from neon isotopic ratios in the mineral samples were also considered in evaluating the neon production cross sections. Results are given in the accompanying table.

Reference: (1) Reedy R. C., Herzog G. F. and Jessberger E. K. (1979) Earth and Planetary Science Letters, 44, p. 341-348.

This work was performed under the auspices of the U. S. Department of Energy by Lawrence Livermore National Laboratory under contract No. W-7405-Eng-48.

Table: Production cross sections for Ne and Xe isotopes by 14.5 MeV neutrons.

Target	Product	Cross Section (mb)
^{23}Na	^{20}Ne	137 ± 7
^{23}Na	^{21}Ne	5.2 ± 0.4
^{23}Na	^{22}Ne	304* ± 15
^{nat}Mg	^{20}Ne	83 ± 5
^{nat}Mg	^{21}Ne	136 ± 7
^{nat}Mg	^{22}Ne	12.2 ± 0.7
^{133}Cs	^{130}Xe	2.4 ± 0.3
^{133}Cs	^{132}Xe	1730 ± 90
^{nat}Ba	^{129}Xe	1.65 ± 0.08
^{nat}Ba	^{130}Xe	0.031 ± 0.002
^{nat}Ba	^{131}Xe	1.79 ± 0.09
^{nat}Ba	^{132}Xe	0.37 ± 0.02
^{nat}Ba	^{134}Xe	0.32 ± 0.02

* Not including ^{22}Ne from ^{22}Na decay

PRODUCTION OF RADIONUCLIDES IN ARTIFICIAL METEORITES IRRADIATED ISOTROPICALLY WITH 600 MeV PROTONS

R.Michel, P.Dragovitsch, P.Englert and U.Herpers, Institut für Kernchemie der Universität zu Köln, Zülpicher Str. 47, D-5000 Köln-1, FRG.

The understanding of the production of cosmogenic nuclides in small meteorites ($R \lesssim 40$ cm) still is not satisfactory. The existing models for the calculation of depth dependent production rates, e.g. /1-6/, do not distinguish between the different types of nucleons reacting in a meteorite. They rather use general depth dependent particle fluxes to which cross sections have to be adjusted to fit the measured radionuclide concentrations. Some of these models not even can be extended to zero meteorite sizes without logical contradictions. Therefore, a series of three thick target irradiations was started at the 600 MeV proton beam of the CERN isochronuous cyclotron in order to study the interactions of small stony meteorites with galactic protons. In contrast to earlier thick target experiments /7/, and references therein, and to recent experiments for the simulation of the GCR irradiation of large meteorites /8/, in these new experiments a homogeneous 4π-irradiation of the thick targets is performed. The irradiation technique used provides a realistic meteorite model which allows a direct comparison of the measured depth profiles with those in real meteorites. Moreover, by the simultaneous measurement of thin target production cross sections one can differentiate beween the contributions of primary and secondary nucleons over the entire volume of the artificial meteorite.

In most earlier thick target experiments only limited aspects of the production of cosmogenic nuclides were studied, i.e. some special radioisotopes or a particular rare gas was measured. In contrast, the new experiments shall provide an universal simulation for a wide variety of cosmogenic nuclides. For this purpose an international collaboration of $\sim$10 laboratories was initiated /9/ providing all necessary scientific and technical means. So radionuclide production is measured by γ-spectrometry instrumentally and by low-level counting and accelerator mass spectrometry after chemical separation, while the rare gases from He to Xe are studied by static mass spectrometry. The measurements are supported by Monte Carlo calculations of the nuclear cascades in the thick targets. Model calculations using the thus derived nucleon fluxes and experimental thin target excitation functions in combination with all the measured thick target production depth profiles then will provide a unification of the classical thin target and thick target approaches for the description of the production of cosmogenic nuclides in small meteorites.

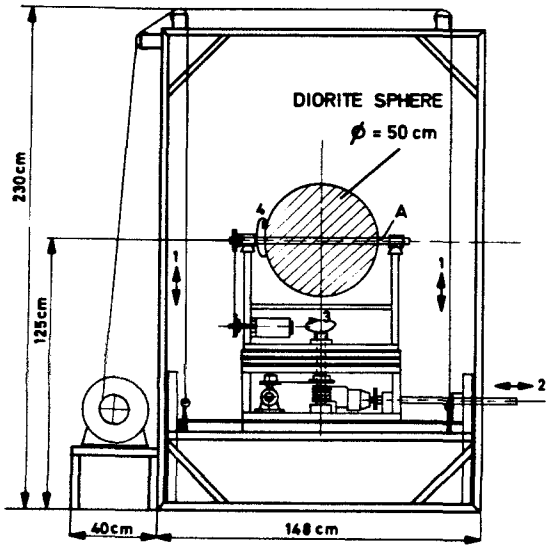

Fig. 1: Experimental set up used for the irradiation of an artifical meteorite with 50 cm diameter. The length of the arrangement was 126 cm.

In the first experiment in Feb. 1983 an artificial meteorite with 10 cm diameter was irradiated and a GCR irradiation age of about 76 My was simulated. A description of this experiment and first results are given elsewhere /10-12/. But the measurements and evaluations are still going on.

In the second experiment an artificial meteorite of 50 cm diameter was irradiated for 12 h with a proton flux of 2.5 μA in Dec. 1983. The homogeneous 4π-irradiation of the target was achieved by a machine (fig. 1) performing 4 independent movements of the artificial meteorite in the beam. Two translational movements (1) and (2) moved the sphere in the indicated directions by 50 cm, each, with velocities of 3.3 cm/min (vertical) and 11. cm/min (horizontal). They simulated a parallel homogeneous proton rain over a 50x50 cm^2 plane. Further the stony sphere made two rotations (3) and (4) with 2 and 5 rpm respectively, thus resulting in a perfect 4π-irradiation. The primary proton flux through the sphere was measured by a 50 cm x 50 cm Al-foil which also made the translational movements and which shadowed the artificial meteorite during irradiation. By the investigation of this Al-foil the homogeneity of the parallel proton rain was proved.

The sphere itself was made out of diorite slabs (ρ=3.0 g/cm^3, $H_2O \leq 10^{-3}$ g/g. It contained a Fe tube (A) with an inner diameter of 1.9 cm. This tube contained 9 Al boxes which were filled with pure element target foils, some chemical compounds and carefully degassed samples of the meteorite JILIN. These targets covered the elements O, Mg, Al, Si, S, Ca, Ti, V, Mn, Fe, Co, Ni, Cu, Zr, Rh, La, Lu, Ba, Te, Au, and Pb. First results are shown in fig. 2. The artificial meteorite received a 600 MeV proton dose of 2.49 x 10^{14} cm^{-2} which is equivalent to a cosmic irradiation age of 4 My. The homogeneity of the irradiation can be seen from the results for Be-7 which - at least from Fe - is exclusively produced by primary particles. The Be-7 profiles from Al and Fe are constant over the entire artificial meteorite within 8.0 % and 3.5 %, respectively. For the other radionuclides the depth profiles show strong increases from the surface to the interior exhibiting important contributions of secondary particles. For Na-22 and Na-24 from Al the increase is by factors of 1.6 and 1.7, respectively. The profiles are fairly symetric. The production of Mn-54 and Co-56 from Fe increases by factors of 1.6 and 1.5.

Co-56 from Fe is of particular interest, since it is exclusively produced by proton induced reactions. Thus the depth profiles of Co-56 from Fe exhibits the action of secondary protons while for Mn-54 and other low energy products reaction of both, secondary protons and neutrons, have to be taken into account.

Generally, the production of Co-56 and Mn-54 from Fe in this meteorite model (fig. 2) are higher than in the sphere with 10 cm diameter (fig. 3). The depth profiles measured for the small sphere show a smaller but still significant increase from the surface to the interior by 20 to 30 %. The generally higher production rates of these nuclides in the big sphere surely are due to the larger amount of secondaries produced in the total targets. For Co-56, however, the maximum production rates are higher by 20 % in the big sphere than in the small one, while for Mn-54 the center production rates even are higher by a factor of 1.6 in the large meteorite model. These first results already demonstrate that in small meteorites the contributions of secondary protons and neutrons are changing with the meteorite sizes and that these

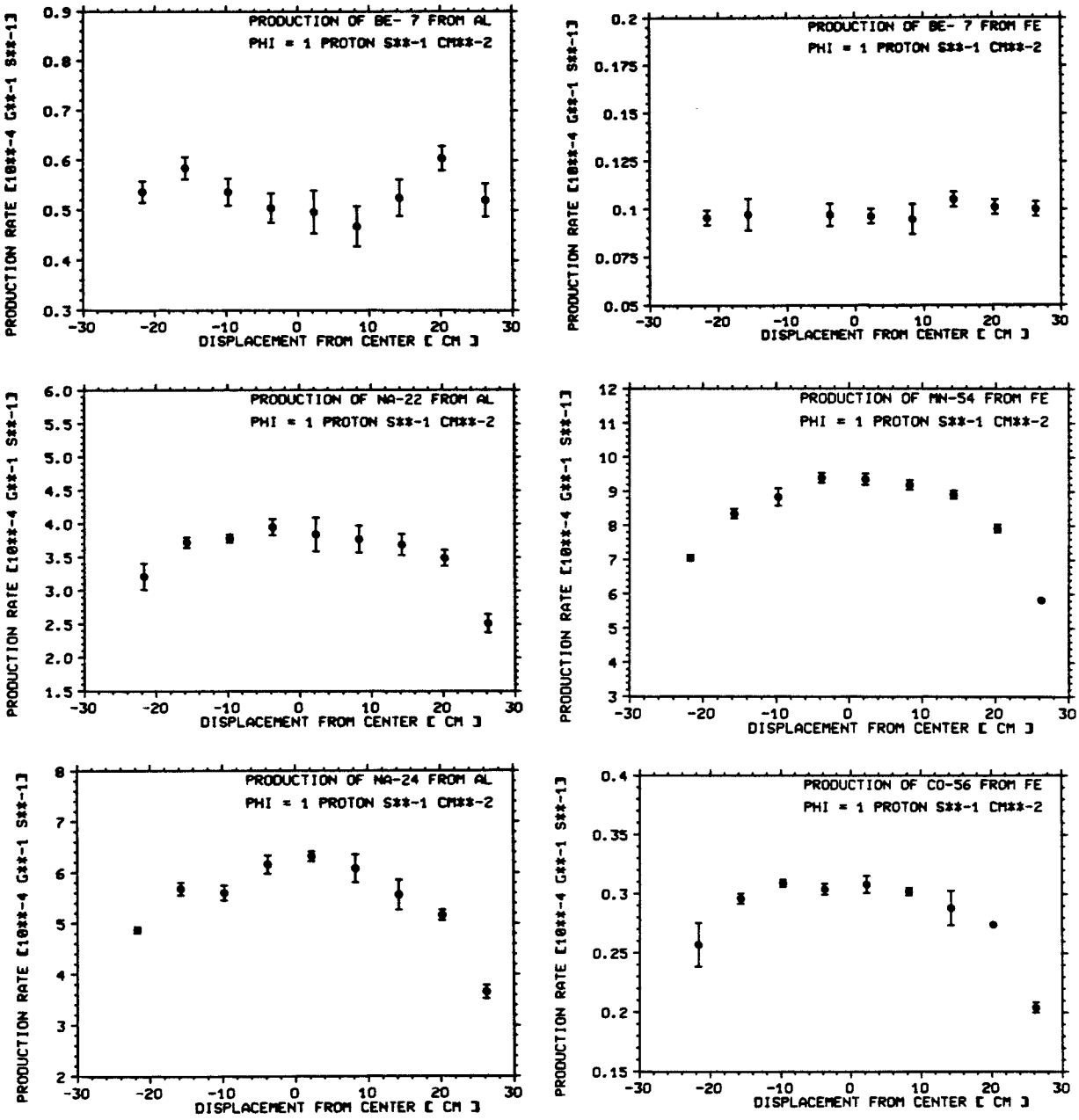

Fig. 2: Depth profiles for the production of radionuclides from Al and Fe in in an artificial meteorite (ρ=3 g/cm^3) with a diameter of 50 cm. The production rates are normalized to a 4π-integrated flux of primary protons of 1 cm^{-2}s^{-1}.

changes are depending on the types of the secondary nucleons.

Consequently, a model describing the production of cosmogenic nuclides in small meteorites has carefully to distinguish between the different types of reacting particles and their depth dependent fluxes. Such a model has to consider the contributions of primary and secondary galactic as well as of solar particles. The interaction of primary solar and galactic cosmic rays with

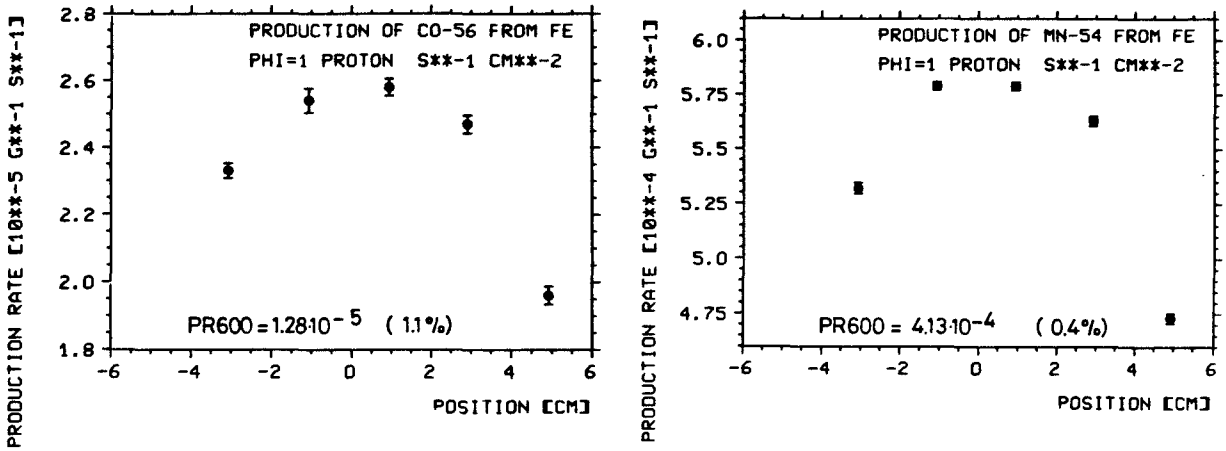

Fig. 3: Depth profiles for the production of Mn-54 and Co-56 from Fe in an artificial meteorite (ρ=3 g/cm^{-3}) with a diameter of 10 cm. The production rates are normalized to a 4π-integrated flux of primary protons of 1 cm^{-2}s^{-1}. The PR 600 values are the production rates due to primary 600 MeV protons only. The errors of these production rates are given in parentheses.

meteorites can be calculated with good a priori accuracy /13,14/. A description of the depth dependent contributions of secondary protons and neutrons will be possible on the basis of the experimental thick target production rates measured in the present simulation experiments.

References

1) J.R.Arnold et al., J.Geophys.Res. 66 (1961) 3519
2) A.K.Lavrukhina and G.K.Ustinova, EPSC 15 (1972) 137
3) R.C.Reedy et al., EPSC 44 (1979) 341
4) S.K.Bhattacharya et al., EPSC 51 (1980) 45
5) M.Bhandari and M.B.Potdar, EPSC 58 (1982) 116
6) R.C.Reedy, LPS XV (1984) 675, and Proc. 15th Lun.Plan.Sci. (1984) in press
7) H.Weigel et al., Radiochimica Acta 21 (1974) 179
8) P.Englert et al., LPS XIV (1983) 175
9) R.Michel for Cologne Collaboration in: "Experiments at CERN in 1983", Geneve Sept. 1983, p 278
10) R.Michel et al., LPS XV (1984) 542
11) S.Theis et al., LPS XV (1984 854
12) P.Englert et al., Nucl.Inst.Methods (1984) in press
13) R.Michel et al., EPSL 59 (1982) 33, ibid 64 (1983) 174
14) R.Michel and R.Stück, J.Geophys.Res. 89, Suppl. (1984) B673

Acknowledgement: This work was supported by the Deutsche Forschungsgemeinschaft

COMPILATION OF COSMOGENIC RADIONUCLIDES IN METEORITES.

K. Nishiizumi, Dept. of Chemistry, B-017, Univ. of Calif., San Diego, La Jolla, CA 92093

Since 1958, when long half-life cosmogenic nuclides in meteorites were first reported, a large amount of data has been published in different journals. The rapid growth in the accumulation of data in the last decade was cuased by two new techniques. The neutron activation method was developed for ^{53}Mn determination. Accelerator mass spectrometry was now widely used for other nuclides. The cosmogenic nuclide data provide much information about the meteorites, especially concerning the last few million years time scale. Some examples are cosmic-ray exposure age, terrestrial age, complex irradiation history, size and depth of the sample in the meteoroid, cosmic-ray intensity and so on. If one combines the cosmogenic radionuclide data and noble gas and cosmic-ray track data, more detailed discussion will be possible. Schultz and Kruse have previously compiled light noble gas data in meteorites [1]. Bhandari et al compiled nuclear track data [2].

I have compiled all available data for the concentration of cosmogenic nuclides $^{53}Mn(t_{1/2} = 3.7\times10^6$ years), ^{26}Al (7.05×10^5 years), ^{10}Be (1.6×10^6 years), ^{36}Cl (3.0×10^5 years) and ^{21}Ne, and $^{22}Ne/^{21}Ne$ ratios in stony, iron, and stony-iron meteorites. For iron meteorites, the $^{4}He/^{21}Ne$ ratio was adopted instead of $^{22}Ne/^{21}Ne$ ratio, because the $^{4}He/^{21}Ne$ ratio in iron meteorites indicates the shielding condition of the sample. The compilation contains over 2000 different analyses for four cosmogenic radionuclides (see Table 1). The list also contains about 200 unpublished data by the author. A preliminary version of the table will be presented at the meeting. Final compilation will be published elsewhere soon. I would be most grateful to receive additional data, published or unpublished.

REFERENCES:

[1] Schultz L. and Kruse H. (1978) Nucl. Track Detection 2, p. 65-103.
[2] Bhandari N., Lal D., Rajan R. S., Arnold J. R., Marti K. and Moore C. B. (1980) Nucl. Track 4, p. 213-262.

TABLE 1

	No. of meteorites	^{53}Mn	^{26}Al	^{10}Be	^{36}Cl
Stony	674	431	839	128	110
Stony-iron	20	27	6	7	31
Iron	89	125	87	55	146
Total	783	583	982	190	287

REDETERMINATION OF PARAMETERS FOR SEMI-EMPIRICAL MODEL FOR SPALLOGENIC He AND Ne IN CHONDRITES. L.E. Nyquist, SN4/NASA Johnson Space Center, Houston, TX 77058 and A.F. McDowell, Lunar and Planetary Institute, 3303 NASA Rd 1, Houston, TX 77058

The semi-empirical model described previously (1,2) satisfactorily reproduced a number of shielding-dependent variations in the relative production rates of spallogenic He and Ne in chondrites. However, data for cores of the Keyes and St. Severin meteorites (3,4) showed a subsurface build-up in ^{3}He which was not predicted with the original model parameters and the model was not pursued. Renewed interest in the preatmospheric size of meteorites, spurred in part by the desirability of understanding the exposure history of the SNC meteorites, justifies redetermination of model parameters.

In the semi-empirical model (5) the production rate of nuclide i is

$$P_i = A_i[e^{-\mu_a d} - B_i e^{-\mu_s d}]$$

where $\mu_j = N\rho\sigma_j/A$, j = a,s. N is Avogadro's number and A and ρ are the average atomic weight and the density, respectively, of the meteoritic material. σ_a and σ_s are the interaction cross sections for primary and secondary cosmic rays, respectively. Values of μ_a and μ_s were obtained by scaling the values determined by (5) for the Grant iron meteorite assuming that σ_a and σ_s are proportional to $A^{2/3}$(1). In principle, these parameters can also be independently determined from the Keyes and St. Severin data. However, this was not attempted since it was found to be possible to fit those data by varying only the A_i and B_i.

Values of A_i and B_i obtained from various applications of the model are summarized in Table 1. It is possible to obtain good fits to the concentration gradients of ^{3}He, ^{21}Ne, and ^{22}Ne with depth and to reproduce the ^{3}He/^{21}Ne vs. ^{22}Ne/^{21}Ne trends in the Keyes and St. Severin meteorites with the same model parameters. It is also possible to reproduce the "Bern line" (6) by varying the size of the model meteoroids. However, in this latter case, different model parameters are required than those which yield fits to the Keyes and St. Severin data. This result is a consequence of the fact that the ^{3}He/^{21}Ne-^{22}Ne/^{21}Ne trends for the individual meteorites do not parallel the "Bern line". It is possible to mimic the general trend of the "Bern correlation" by juxtaposition of a family of lines calculated with the same B_i as used for Keyes and St. Severin by assuming that all meteoroids are similar in size and by varying the values of A_3/A_{21} and A_{22}/A_{21} within the limits given in Table 1 for the "Bern family". One possible physical interpretation of this result is that the effective cosmic ray flux varies for different meteorites, perhaps due to a spatial concentration gradient which affects primarily the lower energy particles.

TABLE 1. MODEL PARAMETERS

	A_3	A_{21}	A_{22}	A_3/A_{21}	A_{22}/A_{21}	B_3	B_{21}	B_{22}
St. Severin	17.6	4.78	4.63	3.68	0.968	0.91	0.97	0.947
Keyes	31.6	8.21	8.29	3.85	1.01	0.91	0.97	0.953
Bern line				3.3	1.04	0.85	0.97	0.954
Bern family				2.4-5.5	0.965-1.11	0.91	0.97	0.953

REFERENCES: (1) Nyquist L.E. (1969) Ph. D. Thesis, Univ. of Minn. (2) Nyquist L.E. (1984) LPS XV, 613. (3) Wright R.J. et al. (1973) JGR 78, 1308. (4) Schultz L. and Signer P. (1976) EPSL 30, 191. (5) Signer P. and Nier A.O. (1960) JGR 65, 2945. (6) Eberhardt P. et al. (1966) Z. Naturforsch. 21A, 414.

CALCULATIONS OF COSMOGENIC NUCLIDE PRODUCTION RATES IN THE EARTH'S ATMOSPHERE AND THEIR INVENTORIES; Keran O'Brien, Environmental Measurements Laboratory, New York, N.Y. 10014

The production rates of cosmogenic isotopes in the Earth's atmosphere and their resulting terrestrial abundances have been calculated, taking into account both geomagnetic and solar-modulatory effects.

The local interstellar flux was assumed to be that of Garcia-Munoz, et al. (1) Solar modulation was accounted for using the heliocentric potential model (2) and expressed in terms of the Deep River neutron monitor count rates. (3) The geomagnetic field was represented by vertical cutoffs calculated by Shea and Smart (4) and the non-vertical cutoffs calculated using ANGRI. (5)

Variations in geomagnetic field strength were modelled by changing the magnitude of the vertical cutoffs in proportion to the change in the magnitude of the geomagnetic field strength.

The local interstellar particle flux was first modulated using the heliocentric potential field. The modulated cosmic-ray fluxes reaching the earth's orbit then interacted with the geomagnetic field as though it were a high-pass filter.

The interaction of the cosmic radiation with the earth's atmosphere was calculated utilizing the Bolztmann transport equation. (6) Spallation cross sections for isotope production were calculated using the formalism of Silberberg and Tsao (7,8) and other cross sections were taken from standard sources.

Inventories were calculated by accounting for the variation in solar modulation and geomagnetic field strength with time. Results for many isotopes, including C-14, Be-7 and Be-10 are in generally good agreement with existing data. The C-14 inventory, for instance, amounts to 1.75 $cm_e^{-2}\ s^{-1}$, in excellent agreement with direct estimates. (9,10)

REFERENCES

1. Garcia-Munoz, M., Mason, G. M. and Simpson, J. A. (1975) Ap. J., 202, pp. 265-275.

2. Gleeson, L. J. and Axford, W. I. (1967) Ap. J., 147, pp. L116-L118.

3. O'Brien, K. and Burke, G. de P. (1973) J. Geophys. Res., 78, pp. 3013-3019.

4. Shea, M. A. and Smart, D. (1967) J. Geophys. Res., 72, pp. 2021-2027.

5. Bland, C. J. and Cioni, G. (1968) Earth Planet. Sci. Lett. 4, pp. 339-405.

6. O'Brien, K. (1975) Natural Radiation Environment II, USERDA rep. CONF-72085, pp. 15-54.

7. Silberberg, R. and Tsao, C. H. (1973) Ap. J. Supplement Series 25, pp. 315-333.

8. Silberberg, R. and Tsao, C. H. (1973) Ap. J. Supplement Series 25, pp. 335-367.

9. Grey, D. (1974) PhD Thesis, Univ. of Ariz., Univ. Microfilms, Ann Arbor, Michigan.

10. Damon, P. E., Lerman, J. C. and Long, A. (1978), Ann. Rev. Earth Planet. Sci., 6, pp. 457-494.

^{10}Be CONTENTS OF SNC METEORITES; D.K. Pal, C. Tuniz[1], R.K. Moniot[2], W. Savin[3], S. Vajda, T. Kruse, and G.F. Herzog, Depts. Chemistry and Physics, Rutgers Univ., New Brunswick NJ 08903. [1]Istituto di Fisica, Univ. degli Studi, Trieste, Italy and Istituto Nazionale Fisica Nucleare, Sez. di Trieste, Italy, [2]Div. Sci. Math., Fordham Univ., New York, NY 10023, [3]Dept. Physics, NJ Inst. Tech., Newark, NJ 07100

Several authors have explored the possibility that the Shergottites, Nakhlites, and Chassigny came from Mars (e.g., 1-3). The spallogenic gas contents of the SNC meteorites have been used to constrain the sizes of the SNC's during the last few million years, to establish groupings independent of the geochemical ones and to estimate the likelihood of certain entries in the catalog of all conceivable passages from Mars to Earth (3-5).

Measurements of the radioactive, cosmogenic nuclides supplement the stable isotope data. The ^{26}Al contents of six of the SNC meteorites are known but their interpretation is complicated by the sensitivity of the ^{26}Al production rate to the bulk Al content, a property that varies more than tenfold among the SNC meteorites. In contrast, differences in chemical composition are expected to induce variations of less than 10% in the ^{10}Be contents (6). Furthermore, the ^{10}Be production rate, P_{10}, varies relatively little over the typical range of meteoroid sizes, i.e., in bodies with preatmospheric radii between 20 and 150 g/cm^2 although it does fall rapidly in larger bodies and rises in the interior of St-Severin-sized objects (7-11). The particular shielding dependence of ^{10}Be makes the isotope a good probe of the irradiation conditions experienced by the SNC meteorites. We have measured the ^{10}Be contents of all the members of the group by using the technique of accelerator mass spectrometry (9). The results appear in Table 1.

Samples. With the possible exception of Chassigny, the samples analyzed for ^{10}Be come from the same meteorite fragments as those analyzed for the noble gases. The ^{26}Al measurements for EETA 79001, ALHA 77005 and Nakhla also refer to the same fragments. The samples of EETA 79001 had been prepared by E. Jarosewich for other purposes. We used about 50 mg of meteorite for each ^{10}Be determination.

Adjustments for Chemical Composition. To remove the effects of chemical composition from the ^{10}Be and ^{21}Ne data we multiplied each one by a chemical normalization factor, C, calculated according to the relation $C=P_{Shergotty}/P_X$. The production rates were obtained from equations and composition data in the literature.

^{10}Be Contents and Shielding. The ^{10}Be contents of Nakhla, Governador Valadares, Chassigny, and probably Lafayette, about 20 dpm/kg, exceed the values expected from irradiation of the surface of a large body. The ^{10}Be data therefore do not support scenario III of Bogard et al. (5), one in which most of the ^{10}Be in the SNC meteorites would have formed on the Martian surface; they resemble rather the ^{10}Be contents found in many ordinary chondrites subjected to 4π exposures. Judging from the calculations of Reedy (10), the meteorites named above orbited for several million years as bodies with radii less than 2 m or so.

^{10}Be Exposure Ages. The uncertainties of the ^{10}Be contents lead to appreciable errors in the ^{10}Be ages, $t_{10} = -1/\lambda \ln(1 - {}^{10}Be/{}^{10}Be_o)$, given in Table 1. Nonetheless, the ^{10}Be ages are consistent with the ^{21}Ne ages calculated assuming conventional, small-body production rates and short terrestrial ages for the finds. We believe that this concordance strengthens the case for at least 3 different irradiation ages for the SNC meteorites (5). Given the similar half-thicknesses of the ^{10}Be and ^{21}Ne production rates, the ratios of

the ^{10}Be and ^{21}Ne contents do not appear consistent with common ages for any of the groups. In view of the general agreement between the ^{10}Be and ^{21}Ne ages it does not seem useful at this time to construct multiple-stage irradiation histories for the SNC meteorites.

REFERENCES 1) Wood, C.A. and Ashwal, L.D. (1981), Proc. 12 Lunar Planet. Sci. Conf., 1359-1375. 2) McSween, H.Y. and Stolper, E.M. (1980), Scientific American 242, 54-63. 3) Wasson, J.T. and Wetherill, G.W. (1979), in Asteroids (Ed. T. Gehrels) Univ. Arizona Press, Tucson, pp. 926-974; Wetherill, G.W. (1984), Meteoritics 19, 1-13. 4) Pepin, R.O. and Becker, R.H. (1984), Lunar Planet. Sci. 15, 637-8. 5) Bogard, D.D., Nyquist L.E. and Johnson, P. (1984), preprint. 6) Pal, D.K., Tuniz, C., Moniot, R.K., Savin, W., Kruse, T.H. and Herzog, G.F. (1984), in preparation. 7) Pal, D.K., Moniot, R.K., Kruse, T.H., Tuniz, C. and Herzog, G.F. (1982), Proc. 5th Int. Conf. Geochron. Cosmochron. Isotope Geol., Nikko Natl. Park, Japan. pp. 300-1. 8) Nishiizumi, K., Arnold, J.R., Elmore, D., Tubbs, L.E., Cole, G. and Newman, D. (1982), Lunar Planet. Sci. 13, 596-7. 9) Moniot, R.K., Kruse, T.H., Savin, W., Hall, G., Milazzo, T. and Herzog, G.F. (1982), Nucl. Inst. Meth. 203, 495-502. 10) Reedy, R.C. (1984), Lunar Planet. Sci. 15, 675-6. 11) Tuniz, C., Smith, C.M., Moniot, R.K., Savin, W., Kruse, T.H., Pal, D.K., Herzog, G.F. and Reedy, R.C. (1984), Geochim. Cosmochim. Acta, in press; Tuniz, C., Moniot, R.K., Savin, W., Kruse, T.H., Smith, C.M., Pal, D.K. and Herzog, G.F. (1984), 3rd Int. Symp. Accelerator Mass Spectrom. Zurich, Switzerland. Abstract. 12) Bogard, D.D., Cressy, Jr., P.J. (1973), Geochim. Cosmochim. Acta 37, 527-546. 13) Hohenberg, C.M., Marti, K., Podosek, F.A., Reedy, R.C. and Shirck, J.R. (1978), Proc. Lunar Sci. Conf., 9th, 2311-2344. 14) Hampel, W., Wanke, H., Hofmeister, H., Spettel, B. and Herzog, G.F. (1980), Geochim. Cosmochim. Acta 44, 539-547. 15) Heymann, D., Mazor, E., and Anders, E. (1968), Geochim. Cosmochim. Acta 32, 1241-1268. 16) Ganapathy, R. and Anders, E. (1969), Geochim. Cosmochim. Acta 33, 775-787. 17) Lancet, M.S. and Lancet, K. (1971), Meteoritics 6, 81-86. 18) Schultz, L. and Kruse, H. (1978), Nucl. Track Detection 2, 65-103.

Table 1. ^{10}Be Contents of SNC Meteorites.

Meteorite	ID[a]	^{21}Ne (10^{-8} cm^{3}STP/g)	Ref.	C_{21}	t_{21}[b] (Ma)	^{10}Be (dpm/kg)	C_{10}	t_{10}[b] (Ma)
Shergotty	U817	0.58	15	1.0	3.2	13±1.5	1	2.2
Zagami	01966,54	0.69	15	0.95	3.6	18.6±2.6	0.99	4.6
ALHA 77005	U/EJ	0.75	5	0.56	2.3	15±3	0.95	2.6
EETA 79001A	U/EJ	0.14	4,5	0.78	0.6	7.8±1.1	0.96	1.0
EETA 79001B	U/EJ	0.12d	5	1.06	0.7	8.5±1.1	0.99	1.2
Nakhla	Me804	3.10	16	0.95	16.3	19.7±3.3	1.02	>5c
Lafayette	Me2116	2.70	16	0.95	14.2	18.1±2.5	1.02	>5c
Governador Valadares	LN	2.10	5	1.0	11.7	25.6±3.6	1.03	>5c
Chassigny	P2523	4.14	17,18	0.53	12.2	20.5±3.1	0.97	>5c

a) We thank the sample donors: LN=L. Nyquist (JSC); Me=E. Olsen (Field Museum); O=R. Hutchinson (Brit. Museum); U=E. Jarosewich (Smithsonian).
b) Assumes P_{10}=21.3 dpm/kg and P_{21}=0.18x10^{-8} cm^{3}STP/g-Ma in Shergotty. Uncertainties in t_{10} range from 25 to 50%.
c) High gas and ^{10}Be contents indicate unreliable ^{10}Be age.
d) Considered doubtful by Bogard et al. (Ref. 5).

STUDIES ON COSMOGENIC NUCLIDES IN METEORITES WITH REGARD TO AN APPLICATION AS POTENTIAL DEPTH INDICATORS

R.Sarafin, U.Herpers and P.Englert
Institut für Kernchemie der Universität zu Köln,
D-5000 Köln 1

R.Wieler and P.Signer
Institut für Kristallographie und Petrographie der ETH Zürich,
CH-8092 Zürich

G.Bonani, M.Nessi, M.Suter and W.Wölfli
Laboratorium für Mittelenergiephysik der ETH Zürich,
CH-8093 Zürich

Measurements of stable and radioactive spallation products in meteorites allow to investigate their histories, especially with respect to the exposure to galactic cosmic ray particles and the pre-atmospheric size of the object. While the concentrations of spallation products lead to the determination of exposure and terrestrial ages, production rate ratios are characteristic for the location of the sample in the meteorite. So, one of the aims of our investigations on meteorites is to obtain depth indicators from suitable pairs of cosmogenic nuclides.

Because of the different depth profiles for nuclide productions it is necessary to determine the concentrations of spallation products in aliquots of a single small sample. Such "same sample" measurements of ^{10}Be and light noble gases were performed on 15 ordinary chondrites (7 H- and 8 L-chondrites) which had been studied previously for ^{26}Al and ^{53}Mn at Cologne [1,2]. ^{10}Be was determined by accelerator mass spectrometry using the AMS-facility at the ETH Zürich, the noble gases were measured by static mass spectrometry. The experimental details are given elsewhere [3], some of the results are summarized in table 1. The errors of the ^{10}Be- and ^{26}Al-values are 3-5%, based on counting statistics. In the case of the ^{22}Ne/^{21}Ne-ratios and the ^{53}Mn-data the errors are estimated to be 2% and 5-10% respectively, including statistical and systematical uncertainties.

Tab. 1: Compilation of data on cosmogenic nuclides from aliquot samples of 15 ordinary chondrites. The production rates were calculated from the ^{21}Ne ages [3] and normalized to chemical composition. (^{10}Be- and Ne-data from [3], ^{26}Al and ^{53}Mn unless otherwise cited cf. [1].)

Meteorite	Class	spall. $^{22}Ne/^{21}Ne$	Production - Rates ^{10}Be [dpm/kg]	^{26}Al [dpm/kg Si_{equ}]	^{53}Mn [dpm/kg Fe]
Armel Yuma	L5	1.155	17.3	354	500
Atwood	L6	1.124	15.9	195	413
Bledsoe	H4	1.087	19.2	251	555
Calliham	L6	1.109	18.2	294	497
Claytonville	L5	1.139	18.3	314	407
Eva	H5	1.113	17.9	241	271
Floyd	H4	1.091	19.9	386	470
Hardtner	L	1.085	17.9	288	181
Kiel	L6	1.251	18.3		317 [2]
Loop	L6	1.118	17.6	309	294
Portales No.3	H4-5	1.077	21.0	311	599
Potter	L6	1.109	17.3	274	440
Seminole	H4	1.096	19.6	329	424
Toulon	H5	1.139	17.7	408	319
Willowdale	H	1.066	18.4	328	492

Since long the ratio $^{22}Ne/^{21}Ne$ has been applied as an indicator for irradiation hardness. The results of our measurements allow to investigate the shielding dependence of the radionuclides mentioned above. As an example the correlation between ^{10}Be production rates (normalized to H-group chemistry [4]) and the shielding parameter $^{22}Ne/^{21}Ne$ is given in figure 1, showing that the ^{10}Be production rates slightly depend on sample depth and/or meteorite size. The corresponding relationship for ^{26}Al shows a similar weak trend whereas ^{53}Mn exhibits a quite strong correlation.

Fig. 1: Shielding dependence of the normalized ^{10}Be production rates [3]

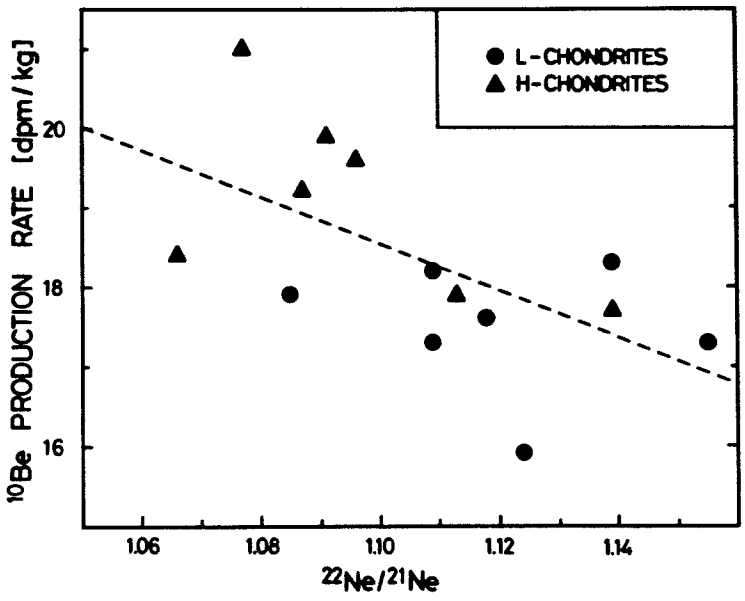

Acknowledgements

The Cologne part of this work was supported by the Bundesministerium für Forschung und Technologie, the Zürich part by the Swiss National Science Foundation, grants No. 2.263-0.81 and 2.443-0.82.

References

[1] U.Herpers and P.Englert (1983) Proc. Lunar Planet.Sci.Conf. 14th, in J.Geophys.Res. 88, B312 - B318 and references cited therein.

[2] P.Englert et al. (1981) Lunar Planet.Sci.XII, 257 - 258.

[3] R.Sarafin et al. (1984) Nucl.Instr. and Meth. (in press).

[4] R.K.Moniot et al. (1983) Geochim.Cosmochim.Acta 47, 1887 - 1895.

THE PRODUCTION RATE OF COSMOGENIC 21-NE IN CHONDRITES DEDUCED FROM 81-KR MEASUREMENTS: L. Schultz and M. Freundel, Max-Planck-Institut für Chem., D-65 Mainz, W-Germany.

Cosmogenic 21-Ne is used widely to calculate exposure ages of stone meteorites. In order to do so, the production rate P(21) must be known. This rate, however, is dependent on the chemical composition of the meteorite as well as the mass of, and position within, the meteoroid during its exposure to the cosmic radiation. Even for a mean shielding the production rates determined from measurements of different radionuclides vary by a factor of two (e.g. [1]).

A method that can be used to determine exposure ages of meteorites that avoids shielding and chemical composition corrections is the 81-Kr-Kr-method. However, for chondrites, in many cases, the direct determination of production rates for the Kr isotopes are prevented by the trapped gases and the neutron effects on bromine. Therefore, we have applied this method to four eucrite falls and then compared their 81-Kr-83-Kr-ages to their cosmogenic 38-Ar concentrations measured in the same samples. The results are given in Tab. 1. From these data a production rate $P(38) = (0.142 \pm 0.005) \times 10^{-8}$ccSTP/gMa for eucrites is deduced. P(21) for these meteorites is calculated from the measured cosmogenic 21-Ne/38-Ar ratios to $(0.188 \pm 0.013) \times 10^{-8}$ccSTP/gMa and the production equation is given by:

$$P(21) = \underset{.18}{1.66}[Mg] + \underset{.2}{0.6}[Al] + \underset{.04}{0.32}[Si] + \underset{.04}{0.22}[Ca] + \underset{.004}{0.023}[Fe,Ni]$$

([X] = concentration of element X as weight fraction)

From this equation P(21) can be calculated for meteorites with other chemical composition. For L-group chondrites a production rate for cosmogenic 21-Ne of $(0.33 \pm 0.04) \times 10^{-8}$ccSTP/gMa is obtained. This value is in good agreement with recently published values [1,4] , but is also considerably lower than the earlier used value of 0.477×10^{-8}ccSTP/gMa 5 .

References: [1] Nishiizumi K. et al. (1980) Earth Planet. Sci. Lett. 50, 156-170. [2] Eugster O. et al. (1967) Earth Planet. Sci. Lett. 2, 77-82. [3] Marti K. (1967) Phys. Rev. Lett. 18, 264-266. [4] Moniot R.K. et al.(1983) Geochim. Cosmochim. Acta 47, 1887-1895. [5] Cressy P.J. and Bogard D.D. (1976) Geochim. Cosmochim. Acta 40, 749-762.

Table 1 : Cosmogenic 38-Ar and 81-Kr/83-Kr-exposure-ages of eucrite falls

Meteorite	38-Ar (10^{-8}cc/g)	81-Kr-age (Ma)
Bouvante	1.01	6.71
	.05	.37
Juvinas	1.35	9.55
	.05	.63
Sioux County	3.03	20.55
	.10	.88
Stannern	5.60; 5.50	42.0, 41.1; 41.8
	.19 .15	2.1 1.3 2.0

NEUTRON CAPTURE PRODUCTION RATES OF COSMOGENIC ^{60}Co, ^{59}Ni AND ^{36}Cl IN STONY METEORITES; M. S. Spergel, York College of CUNY, Jamaica, New York, 11451, USA; R. C. Reedy, Los Alamos National Laboratory, Los Alamos, New Mexico, 87545, USA; O. W. Lazareth and P. W. Levy, Brookhaven National Laboratory, Upton, New York 11973 USA

To unfold the cosmic-ray exposure history of a meteorite, it is best to use a variety of cosmogenic products (tracks and nuclides) with different production profiles. Neutron-capture reactions have production rates which vary considerably with sample depth and meteorite size[1]. Their production profiles differ appreciably from those for tracks or nuclides created by energetic cosmic ray particle spallation reactions. In large meteorites neutron-capture reactions are the main sources of cosmic-ray produced nuclides such as ^{59}Ni and ^{60}Co.[1] The cosmogenic radionuclide ^{60}Co, from the $^{59}Co(n,\gamma)$ ^{60}Co reaction, has been a very useful tool for unfolding the cosmic-ray exposure record of the large Jilin (Kirin) chondrite[2,3].

The neutron-capture reaction rates producing ^{36}Cl, ^{59}Ni, and ^{60}Co in meteorites were calculated by Eberhardt, et al.[1] using neutron slowing-down theory. Lingenfelter et al.[4] used neutron-transport theory to calculate the low-energy neutron flux and neutron-capture induced isotopic anomalies in the moon. Previously we reported neutron-transport theory calculation of the low-energy neutron, as a function of depth, in spherical meteoroids[5] and preliminary results for ^{59}Ni and ^{60}Co production rates.[6-7] Reported here are complete results for neutron flux calculations in stony meteoroids, of various radii and compositions, and production rates for ^{36}Cl, ^{59}Ni, and ^{60}Co.

New neutron source strengths have been calculated that increase our calculated production rates by about 30% in larger meteorites.[11] The $^{59}Ni/^{60}Co$ production ratio in spherical L-chondrites with radii >150 g/cm^2 is usually within agreement with measurements on various large meteorites; but higher than the ratio as calculated by Eberhardt, et al.[1] Neutron-capture calculations for a C3-chrondrite with 100-ppm hydrogen and for an aubrite (≈1% Fe) provide neutron-capture systematics that differ considerably from those obtained with L-chondrites. Measured neutron-capture radionuclides in the Allende meteorite agree better with calculation for a dry chondrite than for one with 100-ppm H; indicating that Allende had a low H content. Our lunar claculations agree with the calculation of Lingenfelter et al.[4], Kornblum et al.[9], and with the lunar neutron measurements.[8] Both the absolute values and the activity-versus-depth profiles calculated for ^{60}Co formation in the Moon agree with the measurements of Wahlen et al.[10] For large spheres the calculated results converge to those obtained for the Moon, but there are significant differences between the lunar results and those predicted for a meteorite with a radius of 1000 g/cm^2. The calculated neutron fluxes and nuclide production rates for small spheres are quite different from those for large meteorites.

The $^{59}Ni/^{60}Co$ ratio is nearly constant with depth in most meteorites: this effect is consistent with the neutron flux and capture cross

section properties. The shape of the neutron flux energy spectrum, varies little with depth in a meteorite. The size of the parent meteorite can be determined from one of its fragments, using the $^{59}Ni/^{60}Co$ ratios, if the parent meteorite was less than 75 g/cm^2 in radius. If the parent meteorite was larger, a lower limit on the size of the parent meteorite can be determined from a fragment. In C3 chondrites this is not possible.

In stony meteorites with R < 50 g/cm^2 the calculated ^{60}Co production rates (mass < 4 kg), are below 1 atom/min g-Co. The highest ^{60}Co production rates occur in stony meteorites with radius about 250 g/cm^2 (1.4 m across). In meteorites with radii greater than 400 g/cm^2, the maximum ^{60}Co production rate occurs at a depth of about 175 g/cm^2 in L-chondrite, 125 g/cm^2 in C3 chrondrite, and 190 g/cm^2 in aubrites. Production results for ^{60}Co and ^{59}Ni in meteorites of radius 300 g/cm^2 (≈86 cm) are shown in Fig. 1 and Fig. 2 respectively. The figures contain results for L Chondrite and C3 type meteorites.

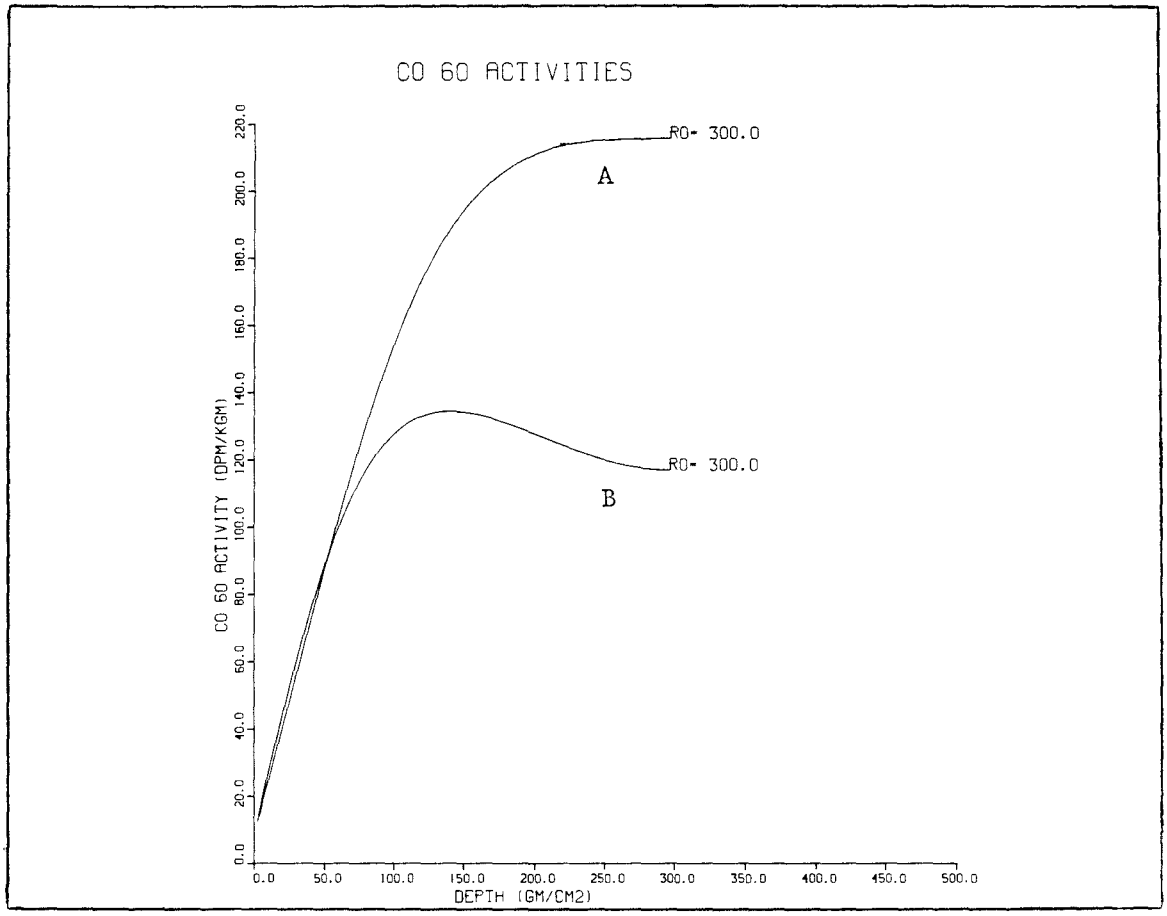

FIG. 1. ^{60}Co production (DPM/Kg) curves in a L Chondrite (A) and a C3 (B). Peak activity occurs closer to the surface in the C3 Chondrite. Cobalt activity levels are effected by the different hydrogen abundances in the meteorites.

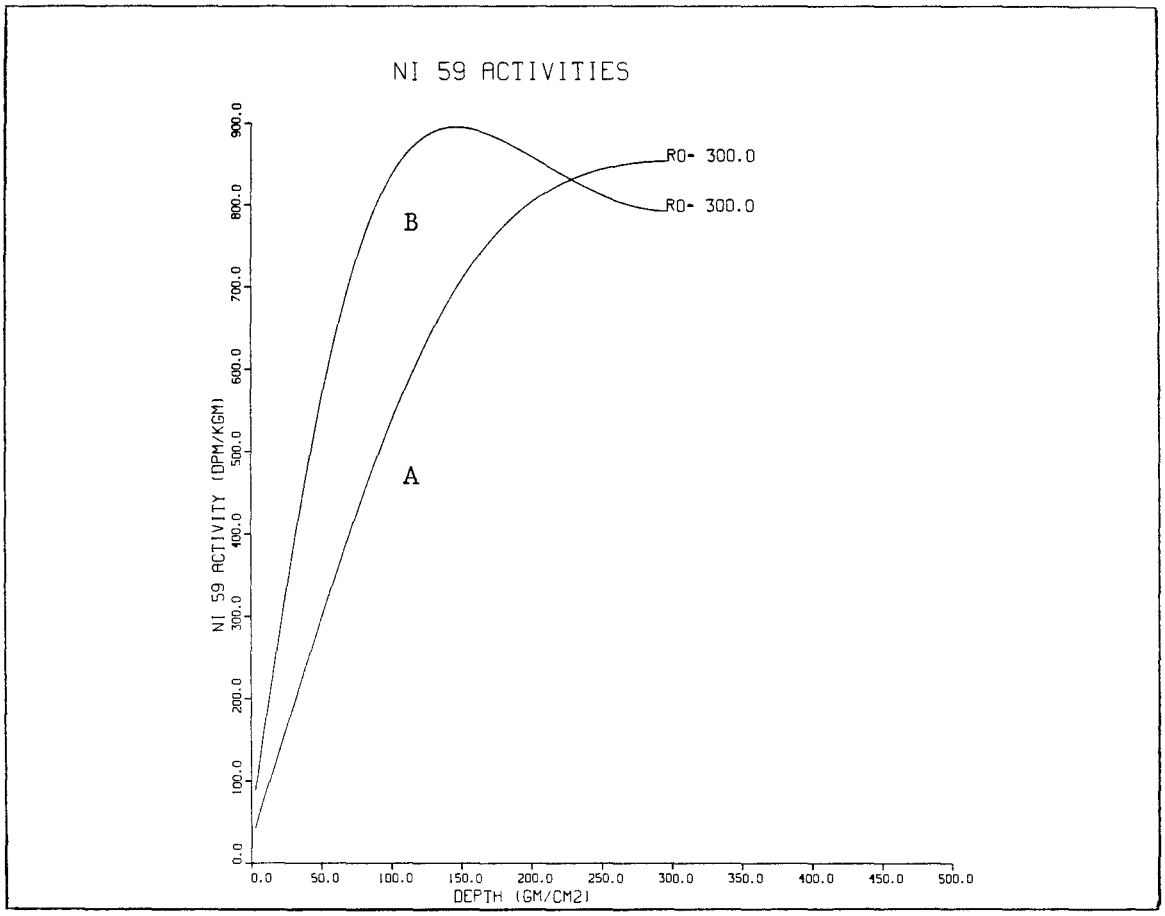

FIG. 2. ^{59}Ni production (DPM/Kg) curves in a L Chondrite (A) and a C3 Chondrite (B). Peak activity occurs closer to the surface with the C3 Chondrite.

1. Eberhardt, P., Geiss, T., and Lutz, M. (1963) Neutrons in meteorites, Earth Sci. and Meteoritics, North Holland, Amsterdam, p. 143-168.
2. Honda, M., Nishiizumi, K., Imamura, T., Takaoka, N., Nitoh, O., Horie, K., and Komura, K. (1982) Earth Planet. Sci. Lett. 57, p. 101-109.
3. Heusser, G. and Ouyang, Z. (1981) Meteoritics 16, p. 326-327.
4. Lingenfelter, R. E., Canfield, E. H., and Hempel, V. E. (1972) Earth Planet. Sci. Lett. 16, p. 355-369.
5. Spergel, M. S., Reedy, R. C., Lazareth, O. W., and Levy, P. W. (1980) Meteoritics, 15, p. 370.
6. Spergel, M. S., Reedy, R. C., Lazareth, O. W., and Levy, P. W. (1981) Meteoritics 16, p. 387-388.
7. Spergel, M. S., Reedy, R. C., Lazareth, O. W., and Levy, P. W. (1982) Lunar and Planetary Science XIII, p. 756-757.
8. Woolum, D. S., Burnett, D. S., Furst, M., and Weiss, J. R. (1975) The Moon 12, p. 231-250.
9. Kornblum, J. J., Fireman, E. L., Levin, M., and Aronson, A. (1973) Proc. Lunar Sci. Conf. 4th, p. 2171-2182.
10. Wahlen, M., Finkel, R. C., Imamura, M., Kohl, C. P., and Arnold, J. R. (1973) Earth Planet. Sci. Lett. 19, p. 315-320.

SIMULATION OF COSMIC IRRADIATION CONDITIONS IN THICK TARGET ARRANGEMENTS

S.Theis, P.Englert, Institut für Kernchemie der Universität zu Köln, Zülpicher Str. 47, D-5000 Köln-1, W.-Germany; R.C.Reedy, INC-11, Los Alamos, National Laboratory, Los Alamos, NM 87545, USA; J.R.Arnold, University of California, San Diego, Department of Chemistry, La Jolla, Ca 92093, USA.

Interpreting abundances of cosmogenic nuclides in meteorites, planetary atmospheres and surfaces in terms of exposure history, shielding parameters and cosmic ray flux requires knowledge of the nuclear reactions that produce them in the object or environment considered.

Bombardment experiments with thin and thick targets with energetic charged particles or particle fields have been performed in order to gain a pool of production data (production rates, ratios, cross sections) for cosmogenic nuclides [1,2,3], of which the stable and the long-lived radioactive species are of special interest as they have been measured in many extraterrestrial samples and are used in evaluating the exposure ages and histories of these bodies [4,5]. In order to correlate the simultation experiments with the systematics of spallogenic nuclide production during exposure to the galactic cosmic radiation, it is necessary to determine long-lived radionuclides as well as stable isotopes in targets from such experiments.

An important point in thick target experiments is to transform the available beam geometry to the isotropic irradiation conditions in space. This can be done by mathematical transformations of the data obtained from static thick targets exposed to focussed monoenergetic beams [6], by defocussing the beam and moving the target in the beam line during the irradiation [7] or by using secondary particle fields for the irradiation as they occur in the interior of extraterrestrial objects [8].

nuclide	$T_{1/2}$	decay mode	carrier amount[mg]	chemical yield[%]	detection method
Be-7	53.29 d	ε	1-2	80-90	G, E_γ = 478 keV
Be-10	1.6×10^6 a	β^-	1-2	80-90	AMS
Na-22	2.607 a	β^+	0.05-0.1	99.99	G, E_γ = 1275 keV
Al-26	7.16×10^6 a	β^+	$\sim$2	60-95	GGC, AMS
Ti-44	47.3 a	ε	$\sim$4	90-95	G, GGC (via Sc-44)
Mn-54	312.2 d	ε	$\sim$3	80-85	G, E_γ = 835 keV
Co-56	78.76 d	ε, β^+	instrumental		G, E_γ = 847, 1238 KeV
Co-57	271.3 d	ε	instrumental		G, E_γ = 122, 136 keV
Co-58	70,78 d	ε	instrumental		G, E_γ = 811 keV
Co-60	5.272 a	β^-	instrumental		G, E_γ = 1173, 1332 keV

Table 1: Nuclear properties of radionuclides determined in this study. In columns 4 and 5 carrier amounts and chemical yields of the applied separation procedures are listed. The determination methods in column 6 are: G: high resolution (low-level) γ-spectroscopy, GGC: γ-γ-coincidence spectroscopy, AMS: accelerator mass spectroscopy.

This study is dedicated to the analysis of long-lived cosmogenic radionuclides produced in pure elemental targets during various simultation experiments by using pure instrumental as well as radiochemical methods (see table 1). The nature of the chemical purification procedures depend on the isotope to be separated. the target material, the interfering isotopes present, and the detection method. Some examples of the applied separation schemes have been published previously [8,9]. In all experiments short-lived isotopes were determined prior to chemistry in most of the target elements by high resolution γ-spectroscopy.

A first set of production data was obtained from a high energy neutron ($E_n \leq 800$ MeV) irradiation at several positions under the LAMPF beam stop (Los Alamos Meson Physics Facility) and is given in table 2. The beam stop environment produces secondary particle and especially neutron fields, which resemble those in planetary surfaces (depth >180 g/cm^2) exposed to the GCA [8]. The samples were exposed in three positions with different absolute neutron fluxes and spectral hardness [9].

The nuclide Ti-44($T_{1/2}$ = 47,3 a) was measured in Ti-targets where it is produced via (n,xn) reactions from all stable Ti isotopes (Ti-46,47,48,49,50). The main target isotope, however, is Ti-48(73.8 %), which contributes via a (n,5n) reaction to the Ti-44 activity. Compared to the (n,4n) product Co-56 from the monoisotopic Co-59 the Ti-44 production rates are one order of magnitude lower for the respective irradiation positions.

Ti-44 could be of special interest in lunar surface samples. It is produced by SCR reactions in the upper layers and - because of its half-life - able to monitor the mean solar activity for at least 4-5 eleven-year solar cycles. As demonstrated, another very important source of Ti-44 in lunar samples are reactions of high energy secondary neutrons with Ti, which has an abundance of several % in the moon [10]. These reactions can occur in greater depths, where the lunar secondary particle cascade is well developed. Here spallation production in iron is of less significance.

product	sample location 2001	2005	2006	ref.
	[accum. atoms g^{-1}]			
Al-26(Al)	1.3×10^{14}	6.4×10^{13}	4.1×10^{13}	[9]
Na-22(Al)	3.2×10^{13}	1.7×10^{13}	8.8×10^{12}	[9]
Be- 7(Al)	1.2×10^{12}	6.7×10^{11}	3.8×10^{11}	[9]
Co-60(Co)	4.4×10^{15}	1.7×10^{16}	2.1×10^{16}	
Co-58(Co)	3.0×10^{14}	1.8×10^{14}	1.0×10^{14}	
Co-57(Co)	1.0×10^{14}	5.7×10^{13}	3.9×10^{12}	
Co-56(Co)	1.6×10^{13}	8.3×10^{12}	---	
Ti-44(Ti)	1.6×10^{12}	1.2×10^{12}	5.2×10^{11}	
Na-22(Ti)	---	1.2×10^{11}	4.9×10^{10}	
Be- 7(Ti)	---	1.8×10^{11}	5.5×10^{10}	
Be- 7(Fe)	2.0×10^{11}	1.4×10^{11}	---	[9]
Na-22(Ni)	2.6×10^{10}	1.8×10^{10}	6.5×10^{9}	[9]

Table 2: Production of low and high energy products in various targets (target elements in brackets) in different irradiation positions under the LAMPF beam stop. For comparison selected results of instrumentally determined Co-isotopes are given.

Another approach to simulate 2-π irradiation conditions of planetary surfaces which has been widely applied in the past are bombardments of so called thick targets [11]. A very large thick target was exposed recently to

2.1 GeV protons at the Bevatron-Bevalac in Berkeley [12]. In a 100x100x180 cm steel surrounded granodiorite target radioactive medium and high energy spalla-products of the incident primary and of secondary particles were analized along the beam axis down to depths of 140 g/cm^2 in targets such as Cu, Ni, Co, Fe, Ti, Si, SiO_2 and Al. Activities of these nuclides were exclusively determined via instrumental γ-ray spectroscopy. Figure 1 shows relative yields of neutron capture and spallation products induced in Co and Cu targets during the thick target bombardment as a function of depth. The majority of the medium energy products such as Co-58 from Co targets exhibit a maximum at shallow depths of 40-60 g/cm^2 and then decrease exponentially.

In a comparable 600 MeV proton bombarded thick target such a slight maximum for medium energy products was not observed [13]. Rather, Co-58 activities in Co decreased steadily with the highest activity at the surface.

The activities of the n-capture product Co-60 increase steadily starting at the surface. This indicates the rapidly growing flux of low energy neutrons ($E_n \leq 1$ keV) within the target. The maximum of the low energy neutron distribution lies between 130 and 170 g/cm^2 [12], which is significantly deeper than in the 600 MeV proton bombarded artificial lunar regolith [3]. Be-7 activities representing high energy spallation in Co decrease, as expected, exponentially with depth.

The comparison of the two experiments shows that both, experimental arrangement and incident particle energy have a significant influence of the results obtained. To gain more insight in the developement of secondary particle fluxes within planetary surfaces which are exposed to an energetically diverse particle field, results of both simulation experiments will be discussed in detail.

References: [1] e.g. R.Michel et al., 1978, J.Inorg.Nucl.Chem. 40, 1845; [2] R.C.Reedy et al., 1979, Earth Planet. Sci.Lett. 44, 341; [3] R.Michel et al., 1974, Radiochim.Acta 21, 169; [4] P.Englert et al., 1978, Geochim.Cosmochim.Acta 42, 1635; [5] S.Regnier et al., 1983, Meteoritics 18, 384; [6] M.Honda, 1962, J.Geophys.Res. 67, 4847; [7] R.Michel et al., 1984, Lun.Planet.Sci. Conf. XV, 542; [8] P.Englert et al., 1983, Lun.Planet.Sci. Conf. XIV, 175; [9] S.Theis et al., 1984, Lun.Planet. Sci.Conf. XV, 855; [10] R.W.Perkins et al., 1970, Proc.Apollo 11 Lun.Sci.Conf., 1455; [11] T.B.Kohmann et al., 1967, In: High Energy Nuclear Reactions in Astrophysics, Benjamin, New York, 169; [12] P.Englert et al., 1983, Meteoritics 18, 294; [13] H.Weigel et al., 1974, Radiochim.Acta 21, 179.

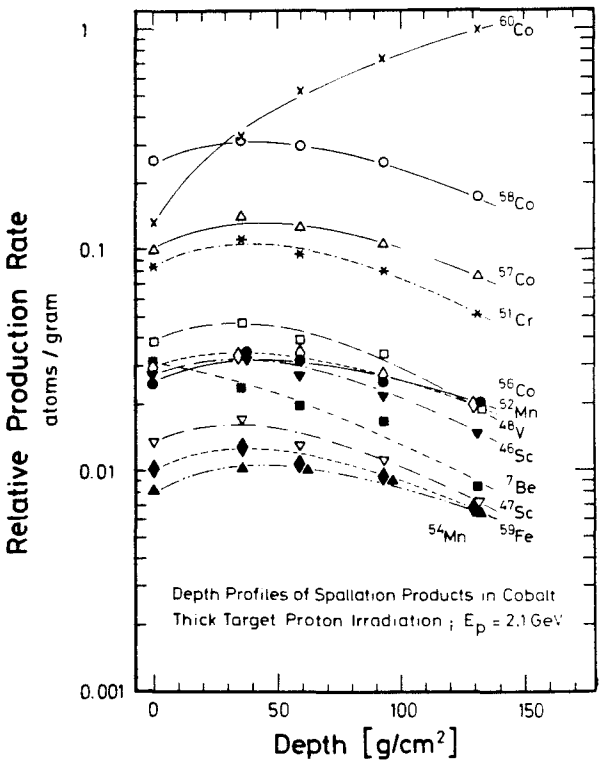

Figure 1

COSMOGENIC RARE GASES AND 10-BE IN A CRACK SECTION OF KNYAHINYA

R. Wieler, P. Signer, ETH Zürich, NO C61, 8092 Zürich, Switzerland; U. Herpers, R. Sarafin, Univ. Köln, Zülpicherstr.47, 5000 Köln, FRG; G. Bonani, H. J. Hofmann, E. Morenzoni, M. Nessi, M. Suter, W. Wölfli, ETH Zürich, HPK, 8093 Zürich, Switzerland

We initiated a study of the concentrations of cosmogenic nuclides as a function of shielding on samples from a "crack section" of the 293 kg main fragment of the L5 chondrite Knyahinya. The stone broke into two nearly symmetrical parts upon its fall in 1866. The planar crack section has diameters between 40 and 55 cm. We measured He, Ne, and Ar on about 20 samples by mass spectrometry and determined the 10-Be activities on aliquots of 10 selected samples by AMS. 26-Al analyses are in progress.

The noble gas data are presented in an abstract for the Met. Soc. Meeting in Albuquerque (1). Here we show the 10-Be data and compare the abundances of spallogenic nuclides with the model calculations reported by Reedy (2) for spherical L chondrites. The figure shows the 10-Be production rates in Knyahinya versus the shielding parameter 22-Ne/21-Ne. Typical errors for 10-Be are $\pm$ 5%. In addition, production rates we determined on 13 individual chondrites (3) are also shown. Noble gases and 10-Be were measured on aliquots in all cases. The 10-Be production rates for H chondrites were normalized to L chondrite chemistry by multiplication with 1.075 (4).

The Knyahinya data are in good agreement with 10-Be determinations on the St. Severin core (5). The slopes of the linear best fits through these two sets of data points are equal within error limits. The 21-Ne/10-Be ratios in Knyahinya are constant within error limits over the whole section, indicating a comparable shielding dependence of the 21-Ne and the 10-Be production rates in this meteorite. In the individual chondrites, the 10-Be production rate appears to depend less on shielding than in Knyahinya. This is similar to the observed variations in a 3-He/21-Ne vs. 22-Ne/21-Ne diagram, where data from the meteorites Keyes and St. Severin do not coincide with the "Bern line" obtained on individual chondrite samples (cf. 1).

The observed noble gas profiles are in fair agreement with Reedys model predictions for a sperical meteoroid of about 150 g/cm^2 (2), if we assume the area of maximum shielding observed in the crack section to correspond to the center of mass of the meteoroid. The postatmospheric surface closest to the meteoroid surface seems to have suffered an ablation of about 20 g/cm2. 10-Be activities in Knyahinya are up to about 25% higher than the largest values to be found according to the calculations in L chondrites of 150 g/cm^2 preatmospheric radius.

Refs: 1) Wieler R. et al. , 1984, abstract, Met. Soc., 47th Ann. Meeting, Albuquerque. 2) Reedy R. C., 1984, Proc. Lun. Planet. Sci. Conf. 15th, to be publ. 3) Sarafin R. et al., 1984, Proc. Symp. AMS' 84, Nucl. Inst. & Methods. 4) Moniot R. K. et al., 1983, Geochim. Cosmochim. Acta 47, 1887. 5) Tuniz, C. et al., 1984, Geochim. Cosmochim. Acta, to be publ.

Work supported by the Swiss National Science Foundation.